Regular article

APOPTOSIS-INDUCING FACTOR MEDIATES DOPAMINERGIC CELL DEATH IN RESPONSE TO LPS-INDUCED INFLAMMATORY STIMULUS. EVIDENCE IN PARKINSON'S DISEASE PATIENTS

M.A. Burguillos[1,2,5], N. Hajji[2,3], E. Englund[4] , A. Persson[4], A. M. Cenci[5], A. Machado[1], J. Cano[1], B. Joseph[2*] and J.L. Venero[1*]

[1]Departamento de Bioquímica y Biología Molecular. Facultad de Farmacia. Universidad de Sevilla, Spain

[2] Department of Oncology-Pathology, Cancer Centrum Karolinska (CCK), R8:03, Karolinska Institutet, SE-171 76 Stockholm, Sweden

[3] Present address: Department of Experimental Medicine and Toxicology, Division of Investigative Science, Imperial College London, United Kingdom.

[4] Department of Pathology, Division of Neuropathology, Lund University Hospital, 221 85 Lund, Sweden.

[5] Present address: Basal Ganglia Pathophysiology Unit, Department of Experimental Medical Science. BMC F11, 22184 Lund, Sweden.

* BJ and JLV share co-seniorship of this paper.

Corresponding author:
Dr. Jose L. Venero
Departamento de Bioquímica y Biología Molecular. Facultad de Farmacia, Universidad de Sevilla, C/ Prof. García González, 2, 41012 Sevilla, Spain
Phone: 0034 954 55 38 03
Fax: 0034 954 55 6752
E-mail: jlvenero@us.es

Abstract

We show that intranigral lipopolysaccharide (LPS) injection, which provokes specific degeneration of DA neurons, induced caspase-3 activation in the rat ventral mesencephalon, which was mostly associated with glial cells. In contrast, nigral DA neurons exhibited AIF nuclear translocation in response to LPS. A significant decrease of the Bcl-2/Bax ratio in nigral tissue after LPS injection was observed. We next developed an *in vitro* co-culture system with the microglial BV2 and the DA neuronal MN9D murine cell lines. The silencing of caspase-3 or AIF by small interfering RNAs exclusively in the DA MN9D cells demonstrated the key role of AIF in the LPS-induced death of DA cells. In vivo chemical inhibition of caspases, Poly(ADP-ribose)polymerase-1, an upstream regulator of AIF release and calpain, proved the central role of the AIF-dependent pathway in LPS-induced nigral DA cell death. We also observed nuclear translocation of AIF in the ventral mesencephalon of Parkinson's disease subjects.

Keywords: apoptosis-inducing factor, caspase 3, apoptosis, Parkinson's disease, substantia nigra, dopamine.

Introduction

Parkinson's disease (PD) affects approximately 1-3% of the population, and is characterised by a slow and progressive degeneration of dopaminergic (DA) neurons in the substantia nigra (SN) (Obeso et al., 2000).

Recent evidence suggests that inflammation may play a central role in the cell loss seen in PD (Hirsch and Hunot, 2009; Tansey et al., 2007). Epidemiological studies have demonstrated convincingly that the incidence of idiopathic PD is lower in chronic users of anti-inflammatory drugs (Chen et al., 2003, 2005; Esposito et al., 2007).

We have previously demonstrated that the intranigral injection of lipopolysaccharide (LPS) selectively induces the death of DA neurons (Castaño et al., 1998). Given the potential role of inflammation in the pathogenesis of PD, the elucidation of the cellular/molecular mechanisms leading to DA cell death in the LPS model is indispensable.

Studies in experimental models and PD patients are suggestive of multiple death pathways including intrinsic and extrinsic apoptosis and autophagy (Levy et al., 2009; Irrcher and Park, 2009). Human postmortem studies suggest that DA neurons die by apoptosis in PD (Hartmann and Hirsch, 2001; Tatton et al., 2003). Fas receptor (Mogi et al., 1996) and autophagic vacuoles (Anglade et al., 1997) were reported to be elevated within the nigrostriatal system of PD patients and in several experimental models of parkinsonism (Fornai et al., 2004). Neural cell death associated with several PD genes, including α-synuclein, parkin, PINK1, DJ-1, and LRRK2, involves caspase activation (Levy et al., 2009). Similarly, the DA neurotoxins MPTP, rotenone, and 6OHDA produce caspase activation and mitochondrial release of cytochrome c (Holtz et al., 2006; Sherer et al., 2002; Turmel et al., 2001). However, the ability of caspase inhibitors to confer protection has been inconsistent (Bilsland et al., 2002; Chu et al., 2005; Hartmann et al., 2001; Liou et al.,2005; Lotharius et al., 1999; Yang et

al., 2004). This observation suggests that alternative death pathways, independent of caspase activation, can be activated in response to injury in nigrostriatal DA neurons.

Apoptosis-inducing factor (AIF) is an apoptotogenic 67-kDa protein that resides in the mitochondrial intermembrane space. After an apoptotic insult, AIF translocates from the mitochondria to the nucleus where the protein induces caspase-independent programmed cell death (Susin et al., 1999). AIF relocalization precedes cell death as indicated by apoptosis-related chromatin condensation and large-scale DNA fragmentation (Hong et al., 2004).

Increasing evidence supports a prominent role of AIF in neurodegeneration. The nuclear translocation of AIF appears to play a key role in cell death regulation in traumatic brain injury (Zhang et al., 2002), oxidative stress (Fonfria et al., 2002), cerebral hypoxia-ischemia (Zhu et al., 2003), epilepsy (Cheung et al., 2005) and Alzheimer's disease (Reix et al., 2007). Consequently, we have undertaken a detailed study with the aim of characterizing the molecular mechanisms leading to the death of nigral DA neurons in the LPS animal model of PD along with examination of autopsy PD patients. Our *in vivo* and *in vitro* data supports a major role of AIF in inducing the death of DA neurons.

Materials and Methods

Animals and lesions – Forty-four male Wistar rats (200-250g), housed in our laboratory, were used for these studies. The rats were anesthetized with 400 mg/kg chloral hydrate and positioned in a stereotaxic apparatus (Kopf Instruments, Tuyunga, CA, USA) to conform to the brain atlas of Paxinos and Watson (1986) and to proceed with the intranigral injection of 2 µl of LPS (1µg/µl). The needle was lowered through a drill hole 5.5 mm posterior, 1.5 mm lateral and 8.3 mm ventral to the bregma for the SN. Monastral blue (Sigma) dissolved in 0.9 % saline served as an inert tracer of the injection site. For experiments involving *in vivo* inhibitors, the animals were divided in five experimental groups (4 animals per group

and postlesion time): (a) One group received 160 mg/kg of benzamide, a selective PARP-1 inhibitor (Sigma), dissolved in saline 60 minutes before intranigral LPS injections and further injected with benzamide every 12 hours intraperitoneally; (b) a second group was injected intranigrally with 1.5 nmol Z-Val-Ala-Asp fluoromethyl ketone (Z-VAD-fmk), a pan caspase inhibitor together with LPS, dissolved in saline containing 0.5% DMSO; (c) a third group was injected intranigrally with LPS together with 1.5 nmol Z-Asp(OMe)-Glu(OMe)-Val-Asp(OMe)-FMK (DEVD-fmk), a specific inhibitor of caspase-3/7 activity, dissolved in saline containing 0.5% DMSO; (d) a fourth group was injected intranigrally with LPS followed by intravenous bolus injection of MDL-28170 (30 mg/kg; 0.5 ml/kg, dissolved in PEG 300 (9):ethanol (1)), (e) a fifth group was injected with LPS intranigrally. Since the different inhibitors were administered under varying conditions, LPS-injected animals were subdivided into three different subgroups. In a first subgroup (n=4), LPS was dissolved in saline, administered intranigrally followed by i.p. saline injections every 12 h. This group was compared with benzamide-injected animals. In a second subgroup (n=4), LPS was dissolved in saline containing 0.5% DMSO and administered intranigrally. This group was compared with those receiving caspase inhibitors; i.e. Z-VAD-fmk- and DEVD-fmk-injected animals. In a third subgroup (n=4), LPS was dissolved in saline, administered intranigrally followed by a single bolus injection of 0.5 ml/kg PEG 300 (9):ethanol (1). This group was compared with MDL-28170-injected animals. The integrity of the nigral DA system was always evaluated 4 days after the intranigral LPS injection. In addition, benzamide treatment was also evaluated 24h after the LPS injection to discard effects on the microglial population. The animals were perfused with 4% of paraformaldehyde under deep anesthesia and their brains were removed and prepared for immunohistological studies. All the experiments were performed in accordance with the guidelines of the European Union

Council (86/609/EU), following the Spanish regulations (BOE 67/8509-12,1988) for the use of laboratory animals and approved by the Scientific Committee of the University of Seville.

Cell culture and treatments - Murine microglial BV2 cell line and murine DA MN9D cell line were used in this study (Joseph et al., 2003). BV2 cells and MN9D cells were cultured and maintained in DMEM media and DMEM/F12 media respectively, both supplemented with 10% FCS, 2 mM L-glutamine, penicillin (100 U/ml) and streptomycin (100 mg/ml). Experiments were performed in reduced 5% FCS media. For the co-culture experiments, MN9D cells (80×10^4 cells/ml) were plated first. The following day, MN9D cells were transfected with lipofectamine 2000 (Invitrogen) following manufacturer's instructions. After 3 hours of transfection, cells were stained with the CellTracker™ Green CMFDA for 30 min, washed three times with PBS and fresh media added. Then BV2 (30×10^4 cells/ml) cells were seeded on them and 1 µM retinoic acid was added to the co-culture to induce cell differentiation. Twenty four hours later, LPS was added (1µg/ml) for another 24 hours. All the knockdown experiments were performed on MN9D cells. For the time-course study of caspase 3 silencing in MN9D cells, experiments were stopped at 48 and 72 hours. The siRNAs used were the following: siRNA against caspase-3 ON-TARGETplus SMARTpool (L-043042-00), ON-TARGETplus SMARTpool Control siRNA Non-targeting siRNA (siRNA NT) #1 (D-001810-01-05) and an oligonucleotide specific for mouse AIF (sense anti-mouse AIF 5'-AUGCAGAACUCCAAGCACGTT-3'.

Human brain

Human brain tissues from patients with PD of 5, 9 and 15 years' duration, and age-matched control cases (cardiac arrest victims, no brain disease) were used in this study. The region investigated was the anterior mesencephalon covering the substantia nigra. They were

microscopically reviewed for verification of pathology and intact morphology, respectively. Prior to the investigation, the entire collection of brain sections, 15-20 per case including the mesencephalic section, were subjected to a neuropathological whole brain analysis for clinical diagnostic purpose, according to routine procedures at the department of Neuropathology. The project procedures involving human brain tissue were approved by the Regional Ethical Review Board in Lund, Sweden.

Western Blot Analysis – Sustantia nigra and cell extracts were processed for immunoblotting. SDS-polyacrylamide gel electrophoresis was performed as described previously (Joseph et al., 2002). Goat polyclonal antibody directed against AIF (Santa Cruz Biotech.), rabbit polyclonal procaspase-3 (Cell Signalling), rabbit polyclonal cleaved PARP (Asp214), rabbit polyclonal Bcl-2 (Santa Cruz Biotech.) and rabbit polyclonal Bax (Santa Cruz Biotech.) were employed. Mouse monoclonal β-actin antibody (Sigma) was used to verify equal loading of the gel. Secondary horseradish peroxidase-conjugated anti-rabbit, anti-goat and anti-mouse antibodies were from Vector labs.

Immunocytochemistry - MN9D cells were stained with CellTracker™ Green CMFDA (Invitrogen) following manufacturer's recommendations for 30 min before co-culture with BV2 cells. Cells were grown on glass slides and fixed with 4% paraformaldehyde during 15 minutes and then washed once with PBS. Cell nuclei were counterstained with Hoechst 33342 (1μg/ml) or DAPI 1μg/ml and apoptotic cell death was quantified as fragmented and/or condensed nuclei of stained neurons, compared to the total number of neurons and with control levels.

Immunohistological studies - Animals were perfused through the heart under deep anaesthesia (chloral hydrate) with 100 ml of PBS containing 10 U/ml heparin followed by

150–200 ml of 4% paraformaldehyde in phosphate buffer, pH 7.4. Brains were removed and then immersed in sucrose in PBS, pH 7.4, first in 10% sucrose for 24 h, 20% sucrose for 24 h and then 30% sucrose until sunk (2–5 days). Tissues were then frozen in isopentane at −15°C and 30 μm sections were cut on a cryostat and mounted in gelatine-coated slices. Primary antibody used was a mouse-derived anti-TH (Chemicon, 1:1000), rabbit-derived anti-AIF (Cell Signaling, 1:50), rabbit-derived anti-cleaved caspase-3 (Cell Signaling, 1:200), mouse-derived anti-OX-6 (Serotec, 1:200), mouse-derived anti-GFAP (Chemicon, 1:300) and rabbit-derived anti Iba1 (Wako, 1:500). All incubations and washes were in PBS, pH 7.4, unless otherwise noted. All work was done at room temperature. Sections were then incubated for 2 h with biotinylated horse anti-mouse or goat anti-rabbit IgG (Vector, 1:200) followed by a second 1-h incubation with ExtrAvidin®-Peroxidase solution (Sigma, 1:100) and for immunofluorescence by a secondary FITC-conjugated anti-rabbit and Texas Red anti-mouse secondary antibody (Vector, 1:200). For colocalization experiments, samples were incubated first either with OX6, GFAP or TH antibodies overnight, and then further incubated with cleaved caspase-3 or AIF antibodies. The different secondary antibodies were then added together.

Confocal studies **-** For time lapse recording, the co-culture was grown in a glass chamber. MN9D was transfected with 1μg of pcDNA3.1 vector expressing enhanced green fluorescent protein (EGFP) with AIF at its C-terminus. Cell nuclei were counterstained with 0.1 μg/ml Hoeschst 33342 (Invitrogen) and a Red- FLICA^{TM} kit for caspase-3 activation (Immunochemistry technologies) was also used. Mitochondria with an intact $\Delta\Psi_m$ were labelled with the potential-dependent dye TMRE (25 nM) (Invitrogen). Chambers were placed in the POC-Chamber/ CTI Controller/ Heating insert P system for live cell imaging. Time–lapse was acquired at 15 minutes intervals for 8 h starting 6h after LPS treatment. A minimum of 100 cells were analyzed (n=3).

Formaldehyde-fixed, paraffin-embedded archival tissue blocks from autopsy on three PD patients and age-matched control cases were analysed at the same time. Four to five sections covering the whole extent of the ventral mesencephalon from its rostral to its caudal pole were used. Immunological analyses using mouse-derived anti-TH (Leica, 1:75), and rabbit-derived anti-AIF (Santa Cruz biotechnology, 1:50) were performed using standard procedures. Alexa 594 conjugated anti rabbit and alexa 488 conjugated anti mouse secondary antibody (1:200) from Invitrogene were used as secondary antibodies. The subcellular localization of AIF protein was determined by laser scanning confocal microscopy. Samples were analyzed under Zeiss 510 Meta confocal laser scanning microscopy equipped with an inverted Zeiss Axiovert 200 m microscope. Mix dyes were acquired by sequential multiple channel fluorescence scanning to avoid bleed through.

Stereological Analysis **-** Quantification of TH-positive cells in the SN was performed according to a modified stereological approach using the Olympus CAST-Grid system. From each animal, sections of 25 µm of thickness were serially cut. Ten of them were systematically sampled from a random starting point along the anterior-posterior axis of the SN region. Thus, the distance between the studied sections was 100 µm. The counted region had a thickness of 1 mm from plate number 37 to plate number 41 of the atlas of Paxinos and Watson (1986). For each section, counting boxes (120 x 90 µm) were placed at three sites equally spaced along the medio-lateral extent of SN. The area of the SN region was estimated using the principle of Cavallieri. All data were collected blind to experimental treatment and expressed as number of neurons per SN.

Quantification of cleaved caspase 3-expressing cells

The phenotypic characterization of cleaved caspase 3-expressing cells in the ventral mesencephalon in response to intranigral LPS was analyzed from immunofluorescence-labelled sections. Double immunofluorence were performed in each section. Thus, cleaved caspase 3 immunofluorescence was combined with either anti OX-6, GFAP or TH antibodies as markers of microglial, astroglial and DApopulations. For each animal, five sections corresponding to plate numbers 39 and 40 of the atlas of Paxinos and Watson (1986) were analyzed. For each section and antibody (red and green), 2 photographs were taken using a 40x magnification lense. The numbers of cleaved caspase 3 immunofluorescence cells were first counted with the aid of a computer-assisted software (touch count) (analySIS®). Then, merged photographs displaying caspase 3 immunoreactivity (red) and either TH, GFAP or OX-6 (green) were used to allow quantification of number of cleaved caspase 3-immunopositive cells specifically in microglial, astroglial and neuronal dopaminergic populations.

Quantification of microglia activation

Reactive microglial, detected as Iba1 immunopositive cells, were counted. For each animal, five sections corresponding to plate numbers 39 and 40 of the atlas of Paxinos and Watson (1986) were analyzed. For each section, 2 photographs were taken using a 20x magnification and microglial cells were counted with the aid of computer-assisted software (analySIS®). Only cells exhibiting typical morphological features of reactive microglia, as defined by Kreutzberg (1996), were considered for the analysis.

Statistical analysis – Results are typically expressed as mean ± SD. Means were compared by One-way ANOVA followed by Bonferroni´s test. Statistical analysis were performed by using the SGPlus 7.1 software.

Results

Western blot analysis of cleaved caspase 3, PARP cleavage, Bcl-2 and Bax

Mitochondrial outer membrane permeabilization is a critical event in caspase-dependent and caspase-independent cell death. Since this process is regulated by the Bcl-2 family of proteins, we first undertook a time-course western blot analysis of Bcl-2 and Bax proteins in nigral tissue in response to LPS at different postlesion times (1, 2, 3 and 4 days). Notably, a robust down-regulation of Bcl-2 protein expression was observed in SN in response to LPS within the first four postlesion days (Figure 1A-B). With regard to the pro-apoptotic protein Bax, there was also a decrease but much lower respect to Bcl-2 (Fig. 1). Consequently, the ratio Bcl-2/Bax was significantly reduced in nigral homogenates in response to intranigral LPS from day 1 (53.6% decrease) to day 4 (78.6%) (Fig.1B). While the balance of anti-apoptotic to pro-apoptotic Bcl-2 proteins dictates cellular fate, it is feasible to predict the involvement of these proteins in the degeneration of nigral DA neurons in response to LPS. The first obvious candidate to test was caspase 3, the main executioner caspase. However, we failed to detect noticeable levels of cleaved caspase 3 in nigral homogenates at the different postlesion times examined (1, 2, 3 and 4 days) after LPS (Fig. 1C). To validate our experimental conditions, we injected two animals with staurosporine in SN and checked for protein levels of cleaved caspase 3 and PARP cleavage in nigral homogenates by western blotting 6 hours after the injection. Significant levels of cleaved caspase 3 were detected in nigral tissue, thus validating our experimental conditions (Fig. 1C). Supporting the lack of involvement of caspase 3 activation in the LPS-induced neurodegenerative events in the ventral mesencephalon, we did not observe cleavage of the caspase-3/7 nuclear substrate Poly(ADP-ribose) polymerase (PARP-1) in response to LPS (Fig. 1C).

Immunohistochemical detection of caspase-3 activation and AIF in the ventral mesencephalon in response to in vivo intranigral LPS injection

Our western blot analysis was clearly suggestive of mitochondrial outer membrane permeabilization in the SN in response to LPS, an event that is responsible for the release of intermembrane space proteins including cytochrome c and AIF. Considering that significant changes of Bcl-2/Bax were detected as early as 24 h after LPS and that degenerative events associated with intranigral LPS injections in the ventral mesencephalon are mostly completed at 4 days postinjection (Castaño et al., 1998), we decided to perform a detailed immunohistochemical study of cleaved caspase 3 and AIF in the ventral mesencephalon 2 days after intranigral LPS injection.

Immunoreactivity for cleaved caspase-3 was found in the lesioned ventral mesencephalon at 48 hours post lesion. It should, however, be noted that most caspase 3 immunoreactivity was restricted to an area close to the needle track highly reminiscent to that showing the presence of reactive microglia. Supporting this view, co-localization studies demonstrated that active caspase-3 was mostly restricted to reactive microglia and in a minor degree to reactive astroglia (Fig 2). This restrictive pattern of caspase 3 activation justifies why we failed to detect cleaved caspase 3 by western blotting in the whole ventral mesencephalon. Further, the occurrence of cleaved caspase 3 in reactive microglia in response to LPS is rather low as compared with that seen after staurosporine (unpublished observations). In comparison with glial cells, cleaved caspase-3 immnoreactivity within DA neurons was found to be minimal (Figs 2 and 3). It was evident the presence of numerous degenerating DA neurons lacking caspase 3 activation 2 days after LPS (Figs 2 and 3). Cell-counting analysis demonstrated that only 5.4 ± 3.2% of total active caspase-3-positive cells co-localised with TH

at 2 days postinjection. In contrast, 57.8 ± 6.6% of total caspase-3-positive cells were of microglial origin and 30.6 ± 4.4 were of astroglial origin.

Since down-regulation of Bcl-2 facilitates the release of mitochondrial AIF into the cytosol, we analysed the subcellular localization of AIF in LPS-induced nigral lesions. After injecting LPS, the nuclear localisation of AIF within degenerating nigral DA neurons could be observed (Fig 3). AIF labeling was not restricted to the DA neurons. However, we failed to detect nuclear localization of AIF within non-DA neurons (Fig. 3).

In vivo inhibition of AIF signaling, but not of caspase-3, confers protection to nigral DA neurons against LPS

In order to confirm that AIF is involved in the death of the DA neurons under conditions of inflammation, a group of LPS-injected animals were treated with benzamide, a PARP-1 inhibitor. The injection of LPS into the left SN decreased the number of TH-positive neurons at 4 days postinjection (Fig. 4) from 9864 ± 1486 to 5721 ± 462.8 ($p<0.01$). Benzamide treatment robustly protected DA neurons from LPS-induced cell death (8284.6 ± 1491.1) (Fig. 4). To discard a direct effect of benzamide on microglia activation, we analysed the microglia population by means of Iba1 immunohistochemistry at 1 day after LPS treatment (Fig. 4). This postlesion time is associated with maximal cytokine production, a microglia activation marker (Stern et al., 2000), that precedes the death of nigral DA neuons. Benzamide treatment failed to alter LPS-induced microglia activation (Fig. 5).

In order to confirm beyond doubt that DA neurons die by a caspase-independent cell death under conditions of inflammation, we performed *in vivo* inhibition of caspases. To achieve this, we used two different chemical inhibitors under in vivo conditions, which were administered together with LPS: i) Z-Val-Ala-Asp -FMK (Z-VAD-fmk), a pan caspase

inhibitor and ii) Z-Asp(OMe)-Glu(OMe)-Val-Asp(OMe)-FMK (DEVD-fmk), a specific caspase-3/7 inhibitor. Specific inhibition of caspase 3/7 activity by DEVD-fmk failed to protect the nigral DA system from LPS toxicity (4423.8 ± 1422.9; $p<0.01$ as compared with controls (Fig. 4). In contrast, the usage of Z-VAD-fmk, a broad spectrum caspase inhibitor significantly protected nigral DA from LPS toxicity (8722.6 ± 412.6). Since Z-VAD-fmk has been reported to inhibit calpain activation at high concentration (Wood and Newcomb, 1999), we next tested if calpain activation would prevent LPS-induced degeneration of DA neurons. Thus, a single bolus of MDL-28170, a calpain inhibitor, was injected in the tail vein immediately after the intranigral LPS injection. MDL-28170 protected nigral DA neurons against LPS toxicity in similar terms of both benzamide and Z-VAD-fmk (8352.6 ± 425.8).

In vitro experiments corroborate AIF involvement in DA neuron death.

To prove that the LPS-induced death pathway in DA neurons is AIF-dependent, we developed an *in vitro* co-culture model. Using the murine microglial BV2 cell line and the murine DA MN9D cell line, MN9D cell survival was checked by immunofluorescence and apoptotic nuclei quantification. Three different independent experiments were conducted. A minimum of 100 cells were analyzed per experiment. Live cell imaging using confocal microscopy demonstrated: i) The addition of LPS provoked the loss of the mitochondrial transmembrane potential $\Delta\Psi_m$ in MN9D cells co-cultured with BV2 microglial cells, a rationale for releasing AIF, ii) AIF is translocated from the mitochondria to the nucleus, iii) AIF translocation precedes the death of DA cells and iiii) DA cell death occurs in absence of caspase-3 activation (see Fig. 6).

To confirm our hypothesis that AIF plays a prominent role in DA cell death under conditions of inflammation, we specifically knocked down caspase-3 or AIF in undifferentiated MN9D cells and quantified the apoptotic nuclei in them after LPS treatment

(Fig 7). 24h after LPS treatment there was a robust decrease in DA neurons survival (Fig 7D, siRNA non-targeting) in our co-culture system. Caspase-3 knockdown showed no protection in undifferentiated DA cell survival against LPS treatment (Fig. 7D, siRNA caspase-3). We next performed a time-course analysis of caspase 3 silencing in MN9D cells to demonstrate that knock down of AIF in our experimental conditions was long-lasting. Our analysis demonstrated that caspase 3 was efficiently silenced at 48 and 72h upon transfection (Fig. 7A). In addition, caspase3 knockdown did not affect MN9D neuronal cells differentiation (Suppl. Fig. 1).

AIF knockdown increased DA cell death in undifferentiated mixed cultures in the absence of LPS treatment (Fig. 7, siRNA AIF). This effect supports the notion that AIF is phylogenetically an old mitochondrial NADH oxidase whose local redox function is essential for optimal oxidative phosphorylation and for an efficient anti-oxidant defense (Modjtahedi et al., 2006). In contrast, AIF knockdown in differentiated MN9D cells show no effect in the absence of the LPS treatment. However and remarkably, differentiated and undifferentiated MN9D cells lacking AIF in co-culture with BV2 cells were resistant to the LPS-induced cell death (Figs. 7 and 8).

Translocation of AIF in PD subjects

Double immunolabeling for TH and AIF and subsequent confocal imaging analysis were performed in the ventral mesencephalon in paraffin sections from three PD patients and three age- and gender-matched healthy control cases. AIF immunolabeling was widely distributed in the ventral mesencephalon of non-PD subjects, with a preferential distribution over the nigral DA neurons (Fig. 9). Distribution of AIF within ventral mesencephalic neurons was strictly cytosolic in control subjects. We failed to detect a single DA neuron exhibiting nuclear AIF

immunolabeling in non-PD subjects. In contrast, scanty but consistent nuclear localisation of AIF within degenerating nigral DA neurons could be observed in PD subjects (Fig. 9).

Discussion

Our data demonstrate that AIF is a key regulator of *in vivo* DA neuronal cell death in response to LPS-induced inflammatory challenge. Analysis of the ventral mesencephalon of PD patients revealed the occurrence of AIF translocation in degenerating DA neurons. Taken together, we provide compelling evidence that AIF plays a significant role in the complex cascade of events leading to selective degeneration of nigral DA neurons.

The LPS-induced inflammatory response provoked a complex cascade of events leading to both caspase-dependent and caspase-independent mechanisms in the SN. Active caspase-3 was predominantly associated with reactive microglia soon after the challenge. The significance of caspase-3 activation in reactive microglia seems to be associated with the early death of resident microglia and infiltrated neutrophils in response to intranigral LPS injection (Ji et al., 2007). On the other hand, degenerating nigral DA neurons exhibited AIF nuclear translocation but not caspase 3 activation in response to LPS treatment. AIF release is associated to increasing mitochondrial outer membrane permeabilization, which is regulated by the Bcl-2 proteins (Chipuk and Green, 2008). Our time-course analysis of protein expression of Bcl-2 and Bax in nigral homogenates after LPS challenge demonstrated that the ratio Bcl-2 to Bax was highly diminished within the first 4 days postlesion, when death of DA neurons takes place. Since the balance of anti-apoptotic to pro-apoptotic Bcl-2 proteins (i.e. Bcl-2 to Bax) dictates cellular fate by increasing mitochondrial outer membrane permeabilization and the pro-apoptotic Bcl-2 member Bax has been mechanistically linked to AIF release (Cregan et al., 2002), we provide compelling evidence that the ventral mesencephalon exhibits biochemical features to ease AIF release under conditions of inflammation.

Using a siRNA-mediated gene knockdown approach, we confirmed, using microglia cells (BV2) and DA neuronal cells (MN9D), in a co-culture setup, that AIF is specifically required for DA neurons to undergo cell death when the co-culture is exposed to LPS. In the same *in vitro* system, the selective silencing of caspase-3 in MN9D cells was unable to prevent the LPS-induced death of DA neurons. Since we could not exclude the possibility that caspase 3 silencing was short-lived due to compensating mechanisms in response to the LPS-induced caspase 3 activation, we next performed a time-course analysis of caspase 3 silencing in MN9D cells. Our analysis demonstrated the effectiveness and lost-lasting silencing of caspase 3 for at least 72h upon transfection, thus excluding the possibility that caspase 3 would reappear during the experimental time window. By doing that, we conclude that caspase 3 is not involved in the LPS-induced death of dopaminergic MN9D cells in co-culture with microglial BV2 cells.

Undifferentiated MN9D cells express tyrosine hydroxylase, release and transport DA, and express voltage-activated sodium channels (Choi et al., 1991). Despite these dopaminergic characteristics, in an undifferentiated form, these cells have a nonneuronal morphology with around cell body generally lacking any process extension. Differentiation of MN9D cells has been shown to alter cell morphology, growth, gene expression and to induce cell cycle arrest in a way that more closely resemble mature SN pars compacta neurons. (Castro et al., 2001; Hermanson et al., 2003). Since the usefulness of MN9D cells in studies of PD may well depend on how closely they resemble mature dopaminergic nigral neurons, we decided to test the effect of AIF silencing on the LPS-induced death of differentiated MN9D cells in co-culture with microglial BV2 cells. Under these conditions, AIF silencing prevented the death of dopaminergic MN9D cells in response to LPS, thus confirming our view that AIF plays a critical role in the integrity of dopaminergic cells in response to LPS-induced inflammatory challenge.

In a next step and in order to demonstrate conclusively that nigral DA neurons die by a caspase-independent AIF-dependent mechanism, we performed *in vivo* chemical inhibition studies using DEVD-fmk, an inhibitor of caspase-3-like activities, Z-VAD-fmk, a pan caspase inhibitor, benzamide, an inhibitor of PARP-1 activity and MDL-28170, a calpain inhibitor. The usage of the broad range caspase inhibitor Z-VAD-fmk protected nigral DA neurons against LPS-induced neurodegeneration. However, the inhibition of caspase-3/7-like activities failed to protect nigral DA neurons under identical experimental conditions. Inhibition of either PARP-1 or calpain activities by benzamide and MDL-28170 conferred a near-complete protection of the nigral DA system. Considering that Z-VAD-fmk is known to inhibit calpain activity besides caspase activities (Wood and Newcomb, 1999), these *in vivo* findings highly suggest that AIF is a key cell death mediator in DA neurons in response to a pro-inflammatory stimulus.

AIF knockdown *per se* increased the death of MN9D DA cells in co-culture with BV2 microglial cells in undifferentiated but not in differentiated MN9D cells in the absence of LPS treatment. However, LPS was ineffective in inducing DA cell death in our co-culture set up in both forms, thus confirming our *in vivo* data. Consequently, AIF showed a dual role in our *in vitro* culture model: anti-apoptotic in the absence of LPS and pro-apoptotic in response to LPS treatment. Supporting this view, AIF has been shown to possess a dual function in the control of stress-induced cell death (Modjtahedi et al., 2006). AIF is a phylogenetically old mitochondrial NADH oxidase whose local redox function is essential for optimal oxidative phosphorylation and for an efficient anti-oxidant defence. It should be noted the extremely high sensitivity of DA cells to respiratory chain complex I deficiency. In fact, MPTP and rotenone, two neurotoxins widely used to develop animal models of PD, are selective complex I inhibitors (Ayala et al., 2007). In agreement with the above, the silencing of AIF induces a reduction in complex I activity in various cell lines along with increased ROS production

(Apostolova et al., 2006), which in turn could increase the susceptibility of cells to apoptotic death trigger. These effects give rise to a plausible explanation for the increased death rate of undifferentiated DA cells transfected with a siRNA targeting AIF, observed in the co-cultures. As already mentioned, differentiation of MN9D cells has been shown to alter cell morphology, growth, gene expression and to induce cell cycle arrest, which may underlie in the observed differences between differentiated and undifferentiated MN9D cells in response to AIF silencing in absence of LPS. An alternative explanation may be related to the antioxidant capacity of retinoic acid, which was used for inducing differentiation of MN9D cells.

It is noteworthy that only a few studies have shown apoptotic-like features in the parkinsonian SN (Anglade et al., 1997; Mochizuki et al., 1996). Other studies, in contrast, have questioned the presence of apoptotic cells in the parkinsonian SN (Dragunow et al., 1995; Kosel et al., 1997; Banati et al., 1998; Wullner et al., 1999; Jellinger , 2000). To our knowledge, our study is the first to show AIF translocation in the ventral mesencephalon of PD patients. If nigral DA cell death does occur by an apoptotic mechanism in PD, detection of these neurons becomes a difficult task, given the relatively slow rate of SN DA cell loss and the rapid clearance of apoptotic cells (Levy et al., 2009). It has been estimated that, at a given time point (1 day), no more than ~ 0.1–0.2% dying cells should be present in the SN of a PD patient (Wullner et al., 1999). Even with these limitations, we found low but significant nigral DA neurons exhibiting AIF translocation to the nucleus, thus supporting an important role of AIF in the death of nigral DA neurons in PD.

The first strong evidence supporting caspase-independent cell death in nigral DA neurons came from a study by Crocker et al. (2003). They demonstrated that calpain inhibition protects nigral DA neurons against MPTP-induced cell death in mice. The second major evidence came from studies developed in mice lacking the PARP-1 gene, which were highly

resistant to MPTP toxicity in terms of nigral DA neuron survival (Mandir et al., 1999). Both mechanisms have been further associated with AIF release; *i.e.* PARP-1 and calpain activation (Yu et al., 2006). In fact, there is a sequential activation of PARP-1, calpain and AIF release, thus suggesting a relationship between both mechanisms (Moubarak et al., 2007). PARP-1 is a DNA damage surveillance molecule and a mediator of cell death after inflammatory processes since it mediates AIF release from mitochondria to cytosol (Yu et al., 2002). However, it should be stressed that PARP-1 activation is clearly linked to inflammation. Different factors have been shown to contribute to the LPS-induced death of nigral DA neurons including interleukin-1β (IL-1β), tumor necrosis factor α (TNF-α) and activation of iNOS and NADPH oxydase activities (Arimoto and Bing, 2003, Gayle et al., 2002; McCoy et al., 2006; Qin et al., 2004). Supporting this view, i) addition of neutralizing antibodies to IL-1β or TNF-α to primary mesencephalic cultures protected dopaminergic neurons to LPS (Gayle et al., 2002); ii) selective in vivo inhibition of TNF-α with XENP345 was partially effective in protecting nigral DA neurons against intranigral LPS injection (McCoy et al., 2006); iii) The same was true with in vivo administration of L-N(G)-nitroarginine, a selective inhibitor of NOS (Arimoto and Bing, 2003). In keeping with this view, we have demonstrated a correlation between LPS-induced formation of peroxynitrites, a highly reactive free radical derived from NO and $O2^{-}$ (Torreilles et al., 1999) with nigral DA cell death (Tomas-Camardiel, 2004). Since one of the best-accepted ways of activating PARP-1 is through peroxynitrite-induced DNA damage (Szabo and Dawson, 1998), we next tested the possibility that PARP-1 activation and subsequent mitochondrial AIF release could be involved in the death of nigral DA neurons. *In vivo* PARP-1 inhibition using benzamide protected nigral DA neurons against LPS-induced neurotoxicity completely, thus supporting the conclusion that the AIF-mediated caspase-independent pathway plays a key role in the death of adult DA neurons in response to inflammation. It has been recently reported that PARP-1 activation induces mitochondrial

Ca2+ dysregulation, which in turn mediates calpain activation and subsequent AIF truncation and translocation to the nucleus (Vosler et al., 2009). Our data argues in favour of this relationship under neurotoxic conditions associated to inflammation.

In conclusion, we provide strong evidence supporting a death role of AIF in experimental and real PD. Elucidating the molecular mechanisms involved in the death of DA neurons in SN is a priority in order to find future pharmacological interventions aimed at slowing down the natural course of the disease.

Acknowledgements: MN9D cells were obtained from Dr. A. Heller (University of Chicago, Chicago, IL, USA). This work was supported by grants from the Spanish Ministerio de Ciencia y Tecnología SAF 2006-04119 and SAF 2009-13778 (JLV), the Swedish Research Council and the Swedish Cancer Society (BJ). M.A.B. was a FPI fellow of Spanish Ministerio de Educación, Cultura y Deporte during the course of this study. Our gratitude to Prof. Alan Boobis for critically reading this manuscript. Also we would like to thank the inestimable help of Dr Modesto Carballo, Dr Albert García, Dr. J.L. Ribas and A. Fernández (Centro de Investigación, Tecnología e Innovación –CITIUS-) for their advices and technical support.

References

Anglade, P., Vyas, S., Javoy-Agid, F., Herrero, M.T., Michel, P.P., Marquez, J., Mouatt-Prigent, A., Ruberg, M., Hirsch, E.C., Agid, Y., 1997. Apoptosis and autophagy in nigral neurons of patients with Parkinson's disease. Histol. Histopathol. 12, 25-31.

Apostolova, N., Cervera, A.M., Victor, V.M., Cadenas, S., Sanjuan-Pla, A., Alvarez-Barrientos, A., Esplugues, J.V., McCreath, K.J., 2006. Loss of apoptosis-inducing factor leads to an increase in reactive oxygen species, and an impairment of respiration that can be reversed by antioxidants. Cell Death Differ. 13, 354-357.

Arimoto, T., Bing, G., 2003. Up-regulation of inducible nitric oxide synthase in the substantia nigra by lipopolysaccharide causes microglial activation and neurodegeneration. Neurobiol. Dis. 12, 35–45.

Ayala, A., Venero, J.L., Cano, J., Machado, A., 2007. Mitochondrial toxins and neurodegenerative diseases. Front. Biosci. 12, 986-1007.

Banati, R.B., Daniel, S.E., Blunt, S.B., 1998. Glial pathology but absence of apoptotic nigral neurons in long-standing Parkinson's disease. Mov. Disord. 13, 221-227.

Bilsland, J., Roy, S., Xanthoudakis, S., Nicholson, D.W., Han, Y., Grimm, E., Hefti, F., Harper, S.J., 2002. Caspase inhibitors attenuate 1-methyl-4-phenylpyridinium toxicity in primary cultures of mesencephalic dopaminergic neurons. J. Neurosci. 22, 2637-2649.

Castano, A., Herrera, A.J., Cano, J., Machado, A., 1998. Lipopolysaccharide intranigral injection induces inflammatory reaction and damage in nigrostriatal dopaminergic system. J. Neurochem. 70, 1584-1592.

Castro, D.S., Hermanson, E, Joseph, B., Wallen, A., Aarnisalo, P., Heller, A., Perlmann, T., 2001. Induction of cell cycle arrest and morphological differentiation by Nurr1 and retinoids in dopamine MN9D cells. J. Biol. Chem. 276: 43277–43284.

Chen, H., Jacobs, E., Schwarzschild, M.A., McCullough, M.L., Calle, E.E., Thun, M.J., Ascherio, A., 2005. Nonsteroidal antiinflammatory drug use and the risk for Parkinson's disease. Ann. Neurol. 58, 963-967.

Cheung, E.C., Melanson-Drapeau, L., Cregan, S.P., Vanderluit, J.L., Ferguson, K.L., McIntosh, W.C., Park, D.S., Bennett, S.A., Slack, R.S., 2005. Apoptosis-inducing factor is a key factor in neuronal cell death propagated by BAX-dependent and BAX-independent mechanisms. J. Neurosci. 25, 1324-1334.

Chipuk, J.E., Green, D.R., 2008. How do BCL-2 proteins induce mitochondrial outer membrane permeabilization?. Trends Cell Biol. 18, 157-164.

Choi, H.K., Won, L.A., Kontur, P.J., Hammond, D.N., Fox, A.P., Wainer, B.H., Hoffmann, P.C., Heller, A., 1991. Immortalization of embryonic mesencephalic dopaminergic neurons by somatic cell fusion. Brain. Res. 552, 67–76.

Chu, C.T., Zhu, J.H., Cao, G., Signore, A., Wang, S., Chen, J., 2005. Apoptosis inducing factor mediates caspase-independent 1-methyl-4-phenylpyridinium toxicity in dopaminergic cells. J. Neurochem. 94, 1685-1695.

Cregan, S.P., Fortin, A., MacLaurin, J.G., Callaghan, S.M., Cecconi, F., Yu, S.W., Dawson, T.M., Dawson, V.L., Park, D.S., Kroemer, G., Slack, R.S., 2002. Apoptosis-inducing factor is involved in the regulation of caspase-independent neuronal cell death. J. Cell Biol. 158, 507-517.

Crocker, S.J., Smith, P.D., Jackson-Lewis, V., Lamba, W.R., Hayley, S.P., Grimm, E., Callaghan, S.M., Slack, R.S., Melloni, E., Przedborski, S., Robertson, G.S., Anisman, H., Merali, Z., Park, D.S., 2003. Inhibition of calpains prevents neuronal and behavioral deficits in an MPTP mouse model of Parkinson's disease. J. Neurosci. 23, 4081-4091.

Dragunow, M., Faull, R.L., Lawlor, P., Beilharz, E.J., Singleton, K., Walker, E.B., Mee, E., 1995. In situ evidence for DNA fragmentation in Huntington's disease striatum and Alzheimer's disease temporal lobes. Neuroreport. 6, 1053-1057.

Esposito, E., Di Matteo, V., Benigno, A., Pierucci, M., Crescimanno, G., Di Giovanni, G., 2007. Non-steroidal anti-inflammatory drugs in Parkinson's disease. Exp. Neurol. 205, 295-312.

Fonfria, E., Dare, E., Benelli, M., Sunol, C., Ceccatelli, S., 2002. Translocation of apoptosis-inducing factor in cerebellar granule cells exposed to neurotoxic agents inducing oxidative stress. Eur. J. Neurosci. 16, 2013-2016.

Fornai, F., Lenzi, P., Gesi, M., Soldani, P., Ferrucci, M., Lazzeri, G., Capobianco, L., Battaglia, G., De Blasi, A., Nicoletti, F., Paparelli, A., 2004. Methamphetamine produces neuronal inclusions in the nigrostriatal system and in PC12 cells. J. Neurochem. 88, 114-123.

Gayle, D.A., Ling, Z.D., Tong, C.W., Landers, T., Lipton, J.W., Carvey, P.M., 2002. Lipopolysaccharide (LPS)-induced dopamine cell loss in culture: role of tumor necrosis factor-α, interleukin-1β, and nitric oxide. Dev. Brain Res. 133, 27-35.

Hartmann, A., Hirsch, E.C., 2001. Parkinson's disease. The apoptosis hypothesis revisited. Adv. Neurol. 86, 143-153.

Hartmann, A., Troadec, J.D., Hunot, S., Kikly, K., Faucheux, B.A., Mouatt-Prigent, A., Ruberg, M., Agid, Y., Hirsch, E.C., 2001. Caspase-8 is an effector in apoptotic death of dopaminergic neurons in Parkinson's disease, but pathway inhibition results in neuronal necrosis. J. Neurosci. 21, 2247-2255.

Hermanson, E., Joseph, B., Castro, D., Lindqvist, E., Aarnisalo, P., Wallen, A., Benoit, G., Hengerer, B., Olson, L., Perlmann, T., 2003. Nurr1 regulates dopamine synthesis and storage in MN9D dopamine cells. Exp. Cell. Res. 288, 324–334.

Herrera, A.J., Castano, A., Venero, J.L., Cano, J., Machado, A., 2000. The single intranigral injection of LPS as a new model for studying the selective effects of inflammatory reactions on dopaminergic system. Neurobiol. Dis. 7, 429-447.

Hirsch, E.C., Hunot, S., 2009. Neuroinflammation in Parkinson's disease: a target for neuroprotection?. Lancet Neurol. 8, 382-397.

Holtz, W.A., Turetzky, J.M., Jong, Y.J., O'Malley, K.L., 2006. Oxidative stress-triggered unfolded protein response is upstream of intrinsic cell death evoked by parkinsonian mimetics. J. Neurochem. 99, 54-69.

Hong, S.J., Dawson, T.M., Dawson, V.L., 2004. Nuclear and mitochondrial conversations in cell death: PARP-1 and AIF signaling. Trends Pharmacol. Sci. 25, 259-264.

Irrcher, I., Park, D.S., 2009. Parkinson's disease: to live or die by autophagy. Sci. Signal. 2, pe21.

Jellinger, K.A., 2000. Cell death mechanisms in Parkinson's disease. J. Neural Transm. 107, 1-29.

Ji, K.A., Yang, M.S., Jeong, H.K., Min, K.J., Kang, S.H., Jou, I., Joe, E.H., 2007. Resident microglia die and infiltrated neutrophils and monocytes become major inflammatory cells in lipopolysaccharide-injected brain. Glia. 55, 1577-1588.

Joseph, B., Marchetti, P., Formstecher, P., Kroemer, G., Lewensohn, R., Zhivotovsky, B., 2002. Mitochondrial dysfunction is an essential step for killing of non-small cell lung carcinomas resistant to conventional treatment. Oncogene. 21, 65-77.

Joseph, B., Wallen-Mackenzie, A., Benoit, G., Murata, T., Joodmardi, E., Okret, S., Perlmann, T., 2003. p57(Kip2) cooperates with Nurr1 in developing dopamine cells. Proc. Natl. Acad. Sci. U. S. A. 100, 15619-15624.

Kosel, S., Egensperger, R., von Eitzen, U., Mehraein, P., Graeber, M.B., 1997. On the question of apoptosis in the parkinsonian substantia nigra. Acta Neuropathol. 93, 105-108.

Kreutzberg, G.W., 1996. Microglia: a sensor for pathological events in the CNS. Trends Neurosci. 19, 312-318.

Levy, O.A., Malagelada, C., Greene, L.A., 2009. Cell death pathways in Parkinson's disease: proximal triggers, distal effectors, and final steps. Apoptosis. 14, 478-500.

Liou, A.K., Zhou, Z., Pei, W., Lim, T.M., Yin, X.M., Chen, J., 2005. BimEL up-regulation potentiates AIF translocation and cell death in response to MPTP. FASEB J. 19, 1350-1352.

Lotharius, J., Dugan, L.L., O'Malley, K.L., 1999. Distinct mechanisms underlie neurotoxin-mediated cell death in cultured dopaminergic neurons. J. Neurosci. 19, 1284-1293.

McCoy, M.K., Martinez , T.N., Ruhn, K.A., Szymkowski, D.E., Smith, C.G., Botterman, B.R., Tansey, K.E., Tansey, M.G., 2006. Blocking soluble tumor necrosis factor signaling with dominant-negative tumor necrosis factor inhibitor attenuates loss of dopaminergic neurons in models of Parkinson's Disease, 26, 9365-9375.

Mandir, A.S., Przedborski, S., Jackson-Lewis, V., Wang, Z.Q., Simbulan-Rosenthal, C.M., Smulson, M.E., Hoffman, B.E., Guastella, D.B., Dawson, V.L., Dawson, T.M., 1999. Poly(ADP-ribose) polymerase activation mediates 1-methyl-4-phenyl-1, 2,3,6-tetrahydropyridine (MPTP)-induced parkinsonism. Proc. Natl. Acad. Sci. U. S. A. 96, 5774-5779.

Mochizuki, H., Goto, K., Mori, H., Mizuno, Y., 1996. Histochemical detection of apoptosis in Parkinson's disease. J. Neurol. Sci. 137, 120-123.

Modjtahedi, N., Giordanetto, F., Madeo, F., Kroemer, G., 2006. Apoptosis-inducing factor: vital and lethal. Trends Cell Biol. 16, 264-272.

Mogi, M., Harada, M., Kondo, T., Mizuno, Y., Narabayashi, H., Riederer, P., Nagatsu, T., 1996. The soluble form of Fas molecule is elevated in parkinsonian brain tissues. Neurosci. Lett. 220, 195-198.

Moubarak, R.S., Yuste, V.J., Artus, C., Bouharrour, A., Greer, P.A., Menissier-de Murcia, J., Susin, S.A., 2007. Sequential activation of poly(ADP-ribose) polymerase 1, calpains, and Bax is essential in apoptosis-inducing factor-mediated programmed necrosis. Mol. Cell. Biol. 27, 4844-4862.

Obeso, J.A., Rodriguez-Oroz, M.C., Rodriguez, M., Lanciego, J.L., Artieda, J., Gonzalo, N., Olanow, C.W., 2000. Pathophysiology of the basal ganglia in Parkinson's disease. Trends Neurosci. 23, S8-19.

Paxinos, G., Watson, C., 1986. The Rat Brain in Stereotaxic Coordinates. Academic Press, San Diego.

Reix, S., Mechawar, N., Susin, S.A., Quirion, R., Krantic, S., 2007. Expression of cortical and hippocampal apoptosis-inducing factor (AIF) in aging and Alzheimer's disease. Neurobiol. Aging. 28, 351-356.

Sherer, T.B., Betarbet, R., Stout, A.K., Lund, S., Baptista, M., Panov, A.V., Cookson, M.R., Greenamyre, J.T., 2002. An in vitro model of Parkinson's disease: linking mitochondrial impairment to altered alpha-synuclein metabolism and oxidative damage. J. Neurosci. 22, 7006-7015.

Stern, E.L., Quan, N., Proescholdt, M.G., Herkenham, M., 2000. Spatiotemporal induction patterns of cytokine and related immune signal molecule mRNAs in response to intrastriatal injection of lipopolysaccharide. J. Neuroimmunol. 109, 245-260.

Susin, S.A., Lorenzo, H.K., Zamzami, N., Marzo, I., Snow, B.E., Brothers, G.M., Mangion, J., Jacotot, E., Costantini, P., Loeffler, M., Larochette, N., Goodlett, D.R., Aebersold, R., Siderovski, D.P., Penninger, J.M., Kroemer, G., 1999. Molecular characterization of mitochondrial apoptosis-inducing factor. Nature. 397, 441-446.

Szabo, C., Dawson, V.L., 1998. Role of poly(ADP-ribose) synthetase in inflammation and ischaemia-reperfusion. Trends Pharmacol. Sci. 19, 287-298.

Tansey, M.G., Goldberg, M.S., 2009. Neuroinflammation in Parkinson's disease: Its role in neuronal death and implications for therapeutic intervention. Neurobiol. Dis.

Tansey, M.G., McCoy, M.K., Frank-Cannon, T.C., 2007. Neuroinflammatory mechanisms in Parkinson's disease: potential environmental triggers, pathways, and targets for early therapeutic intervention. Exp. Neurol. 208, 1-25.

Tatton, W.G., Chalmers-Redman, R., Brown, D., Tatton, N., 2003. Apoptosis in Parkinson's disease: signals for neuronal degradation. Ann. Neurol. 53 Suppl 3, S61-70; discussion S70-2.

Tomas-Camardiel, M., Rite, I., Herrera, A.J., de Pablos, R.M., Cano, J., Machado, A., Venero, J.L., 2004. Minocycline reduces the lipopolysaccharide-induced inflammatory reaction, peroxynitrite-mediated nitration of proteins, disruption of the blood-brain barrier, and damage in the nigral dopaminergic system. Neurobiol. Dis. 16, 190-201.

Turmel, H., Hartmann, A., Parain, K., Douhou, A., Srinivasan, A., Agid, Y., Hirsch, E.C., 2001. Caspase-3 activation in 1-methyl-4-phenyl-1,2,3,6-tetrahydropyridine (MPTP)-treated mice. Mov. Disord. 16, 185-189.

Vosler, P.S., Sun, D., Wang, S., Gao, Y., Kintner, D.B., Signore, A.P., Cao, G., Chen, J., 2009. Calcium dysregulation induces apoptosis-inducing factor release: cross-talk between PARP-1- and calpain-signaling pathways. Exp. Neurol. 218, 213-220.

Wood, D.E., Newcomb, E.W., 1999. Caspase-dependent activation of calpain during drug-induced apoptosis. J. Biol. Chem. 274, 8309-8315.

Wullner, U., Kornhuber, J., Weller, M., Schulz, J.B., Loschmann, P.A., Riederer, P., Klockgether, T., 1999. Cell death and apoptosis regulating proteins in Parkinson's disease--a cautionary note. Acta Neuropathol. 97, 408-412.

Yang, L., Sugama, S., Mischak, R.P., Kiaei, M., Bizat, N., Brouillet, E., Joh, T.H., Beal, M.F., 2004. A novel systemically active caspase inhibitor attenuates the toxicities of MPTP, malonate, and 3NP in vivo. Neurobiol. Dis. 17, 250-259.

Yu, S.W., Andrabi, S.A., Wang, H., Kim, N.S., Poirier, G.G., Dawson, T.M., Dawson, V.L., 2006. Apoptosis-inducing factor mediates poly(ADP-ribose) (PAR) polymer-induced cell death. Proc. Natl. Acad. Sci. U. S. A. 103, 18314-18319.

Yu, S.W., Wang, H., Poitras, M.F., Coombs, C., Bowers, W.J., Federoff, H.J., Poirier, G.G., Dawson, T.M., Dawson, V.L., 2002. Mediation of poly(ADP-ribose) polymerase-1-dependent cell death by apoptosis-inducing factor. Science. 297, 259-263.

Zhang, X., Chen, J., Graham, S.H., Du, L., Kochanek, P.M., Draviam, R., Guo, F., Nathaniel, P.D., Szabo, C., Watkins, S.C., Clark, R.S., 2002. Intranuclear localization of apoptosis-inducing factor (AIF) and large scale DNA fragmentation after traumatic brain injury in rats and in neuronal cultures exposed to peroxynitrite. J. Neurochem. 82, 181-191.

Zhu, C., Qiu, L., Wang, X., Hallin, U., Cande, C., Kroemer, G., Hagberg, H., Blomgren, K., 2003. Involvement of apoptosis-inducing factor in neuronal death after hypoxia-ischemia in the neonatal rat brain. J. Neurochem. 86, 306-317.

Figure Legends

Figure 1: Time-course analysis of Bcl-2, Bax (A,B), caspase 3 (C) and PARP cleavage (C) in the ventral mesencephalon in response to intranigral LPS injection. Positive control for cleaved PARP and cleaved caspase 3 was made from a 6 hour- treated ventral mesencephalon with 2µl of a 2 mM stock solution of staurosporine (STS)

Figure 2: Analysis of caspase-3 activation in the ventral mesencephalon in response to intranigral LPS injection. Caspase-3 activation was investigated 48 hours after LPS injection in dopaminergic neurons (A-C), astroglia (D-F) and reactive microglia (G-I). A cleaved caspase-3 (Asp175) antibody was employed to detect endogenous levels of the large fragment of active caspase-3 (A, D, G). TH, GFAP and OX-6 immunostaining were used to detect dopaminergic neurons (B), astroglia (E) and reactive microglia (H) respectively. Merge pictures are presented in panel C, F and I. White arrows show examples of no colocalizations between cleaved caspase 3 and degenerating dopaminergic neurons. Scale bar: (A, B, C, G, H and I): 30 µm; (D, E and F): 12 µm.

Figure 3: Upper panel (A-O) shows high magnification photographs of AIF and TH in the ventral mesencephalon in sham (A-E) and in experimental animals 48h after intranigral LPS (F-O). Lower panel (P-Y) shows high magnification photographs of cleaved caspase 3and TH in the ventral mesencephalon in sham (P-T) and in experimental animals 48h after intranigral LPS (U-Y)). Nuclei were labelled with Hoechst. Translocation of AIF into the nucleus of degenerating neurons can be seen after LPS treatment (see white arrows in G-I and L-N). Note how a degenerating dopaminergic neuron in (I) lacks typical morphological features of a healthy neurons (compare with D), which is further exacerbated in (N). Note how these degenerating neurons exhibit nuclear AIF translocation (H and M). Panels A-E

show a typical nuclear-free AIF immunostaining within a healthy dopaminergic neuron. Note how no colocalization of cleaved caspase 3 was detected in degenerating dopaminergic neurons (U-Y; see white arrows). Scale bar: 24μm.

Figure 4: In vivo inhibition of PARP-1 and calpain but not caspase-3/7 protects nigral dopaminergic neurons from LPS-induced cell death. Tyrosine hydroxylase immunohistochemistry in the ventral mesencephalon of control unlesioned animals (Sham animals) (A,B), LPS-injected animals (C, D), LPS+DEVD-fmk-injected animals (E, F), LPS+zVADfmk-injected animals (G,H), LPS+benzamide-injected animals (I,J) and LPS+MDL28170 animals (K,L). Animals were evaluated four days after LPS injection. Scale bar: (A, C, E, G, I, K):260 μm; (B, D, F, H, J, L): 65 μm.

Figure 5: Benzamide treatment failed to alter LPS-induced microglial activation. Iba1 immunohistochemistry in the ventral mesencephalon 24 hours after LPS (A) and LPS+ benzamide (B). (C) Quantitation of microglial cell activation demonstrating null effect of benzamide on LPS-induced microglia activation. Scale bar: 300 μm.

Figure 6: AIF, but not caspase-3, is required for LPS-induced dopaminergic neuron death in BV2/MN9D co-cultures. Panel A shows a time-course screening of living cells demonstrating loss of mitochondria's transembrane potential (ΔΨm) (red labelling) in dopaminergic neurons (green labelling), which precedes its further death. MN9D dopaminergic cells were stained using CellTracker™ Green CMFDA. Mitochondria presenting an intact ΔΨm are stained with the mitochondrial potential-sensitive dye TMRE (red). Addition of LPS to the culture led to the loss of ΔΨm in MN9D cells. Notice the loss of red staining of ΔΨm in a green dopaminergic neurons (see white arrow) flanked by

several microglial cells at 45 min (A) and membrane blebbing at 60 min (A). Note that red TMRE staining in green-labelled neuronal cells turned into orange (see arrow in panel A). In panel B, MN9D DA cells were transfected with vector encoding GFP-tagged AIF and seeded together with BV2 cells. Cell nuclei were stained with 0.1 µg/ml Hoechst 33342 and an aliquot of Red- FLICA^{TM} kit for caspase-3 activation was added to the media. Upon LPS exposure, whereas the release of AIF from mitochondria was observed in the dying neurons, no caspase-3 like activities could be detected (see temporal course in panel B). Note how two DA cells expressing AIF (a and b) are gradually loosing green labelling, an indication of mitochondrial AIF release to start exhibiting features of nuclear condensation and cell death. Cell labelled as (c) in panel B is of microglial origin which possesses active caspase 3/7 activity as labelled in red. In panel C, MN9D DA neuronal cells were cotransfected with an expression vector encoding EGFP tagged AIF (green) and the mitochondrial marker DsRed Mito (red). MN9D cells were then co-cultured with microglia BV2 cells and the co-culture treated with LPS. Representative confocal images of GFP-AIF, mitochondrial DsRed staining and nuclear Hoechst 33342 staining in untreated (C, left panel) and LPS treated co-culture (C, right panel) are shown and analyzed the localization of the three channels using the confocal software. Notice how in the left panel, green and red channel (for AIF and mithocondria respectively) appear together, while in the right panel the green channel mostly coincides with the blue channel (nucleus) and barely with the red channel (mitochondria).

Figure 7: Knock-down of AIF but not of caspase 3 in undifferentiated MN9D DA cells protects them in a co-culture set up with microglia BV2 cells in response to LPS. Panel A shows a time-course experiments of knock-down of caspase 3 at 48 and 72 hour in dopaminergic MN9D cells. Immunoblots of caspase-3 and AIF demonstrate the efficient suppression of their expression upon knockdown with siRNA (A and B). Representative

pictures of the MN9D-BV2 cells co-culture, where MN9D cells were stained with the CellTracker™ Green CMFDA showing condensed nuclei after LPS treatment (C). Panel D shows the quantification of the condensed nuclei in CellTracker™ Green expressing DA neurons in untreated and LPS treated co-cultures upon silencing in MN9D cells of caspase-3 or AIF. Non-targetting siRNA (siRNA NT) was used as control and β-actin used as a protein loading control. Statistical significance: *: $p<0.01$.

Figure 8: Knock-down of AIF reduced apoptotic cell death of differentiated MN9D cells in co-culture with BV2 cells in response to LPS. MN9D apoptotic cell death was assessed by immunostaining (A). siRNAs were directed against AIF or against Non-Targeting gene (siRNA NT) in MN9D cells. Cells were stained with the CellTracker™ Green CMFDA before co-culture with BV2 cells, differentiated with 1 µM retinoic acid and exposed to LPS or not. After fixing the cells, AIF was stained red with Alexa Fluor 594 and nuclei were stained with 1 µg/ml DAPI. White arrows indicate MN9D knock-out AIF cells, "G" letter indicates microglia cells (BV2) and "A" letter indicates apoptotic MN9D cells (A). Black bars represent siRNA against AIF and gray bars represent siRNA NT. Both bars indicate the percentage of MN9D apoptotic cell death. Bars represent the mean ± standard for three individual experiments. *$p < 0.01$ compared to siRNA NT.

Figure 9: Nuclear AIF translocation in substantia nigra dopaminergic neurons from PD subjects. High magnification photographs of TH (green) and AIF (red) in the ventral mesencephalon in in paraffin sections from age- and gender-matched healthy control cases (A-C) and two PD patients (D-I). Merge pictures for every case is depicted (right column). Higher magnification photographs are provided for the PD cases to ease visualization of AIF translocation. Scale bar: (A-C): 80 µm; (D-I): 40 µms.

Supplementary Figure 1: Differentiation of MN9D cells is maintained at 48h and 72h after caspase3 knockdown. siRNAs were directed against caspase3 (siRNA C3) or not (non-targeting siRNA; siRNA NT) for 24h. Then, MN9D cells were differentiated with 1 µM retinoic acid for 24 h. Photographs were taken at 48h and 72h after siRNA transfection.

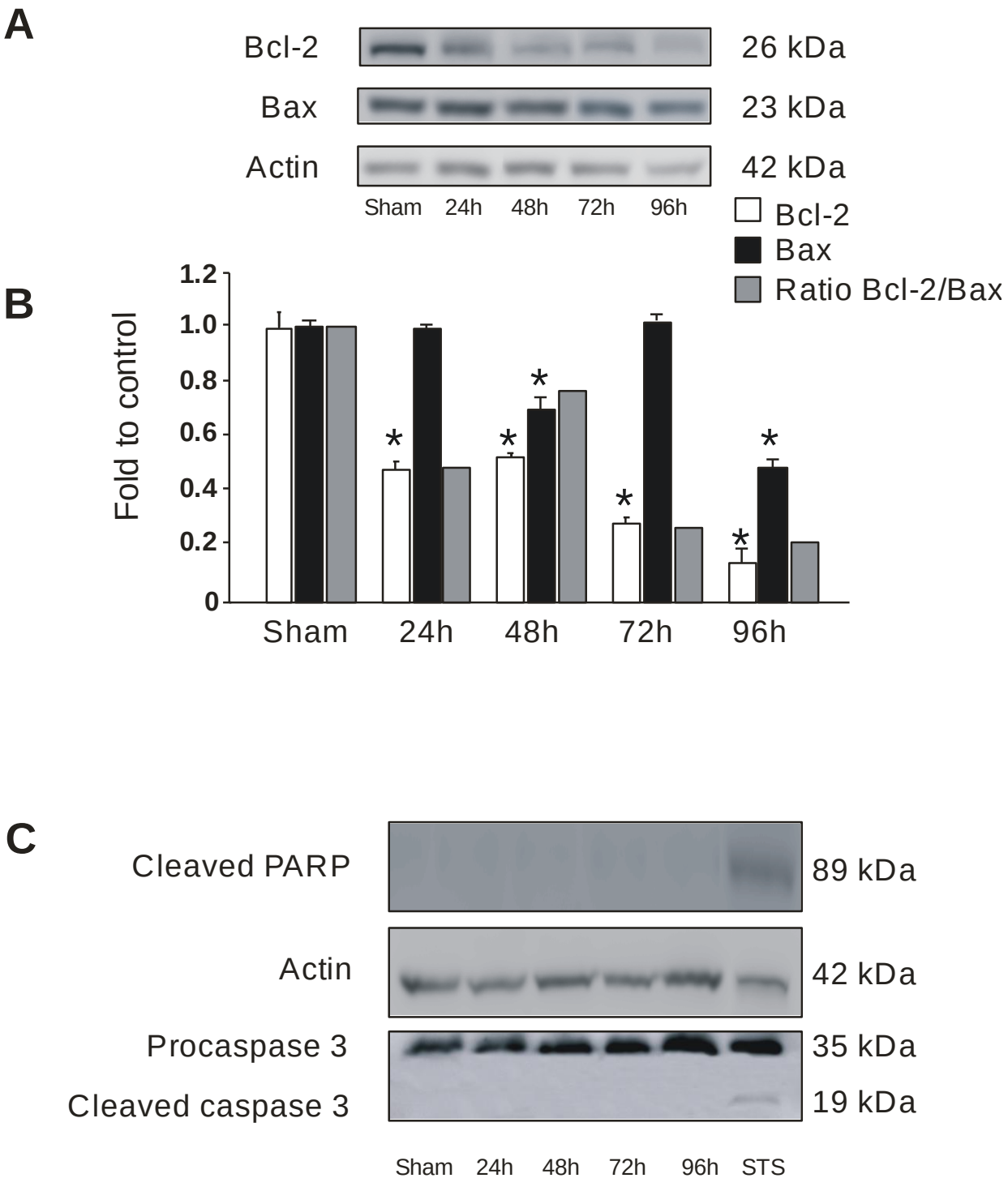

Figure 1. Burguillos et al

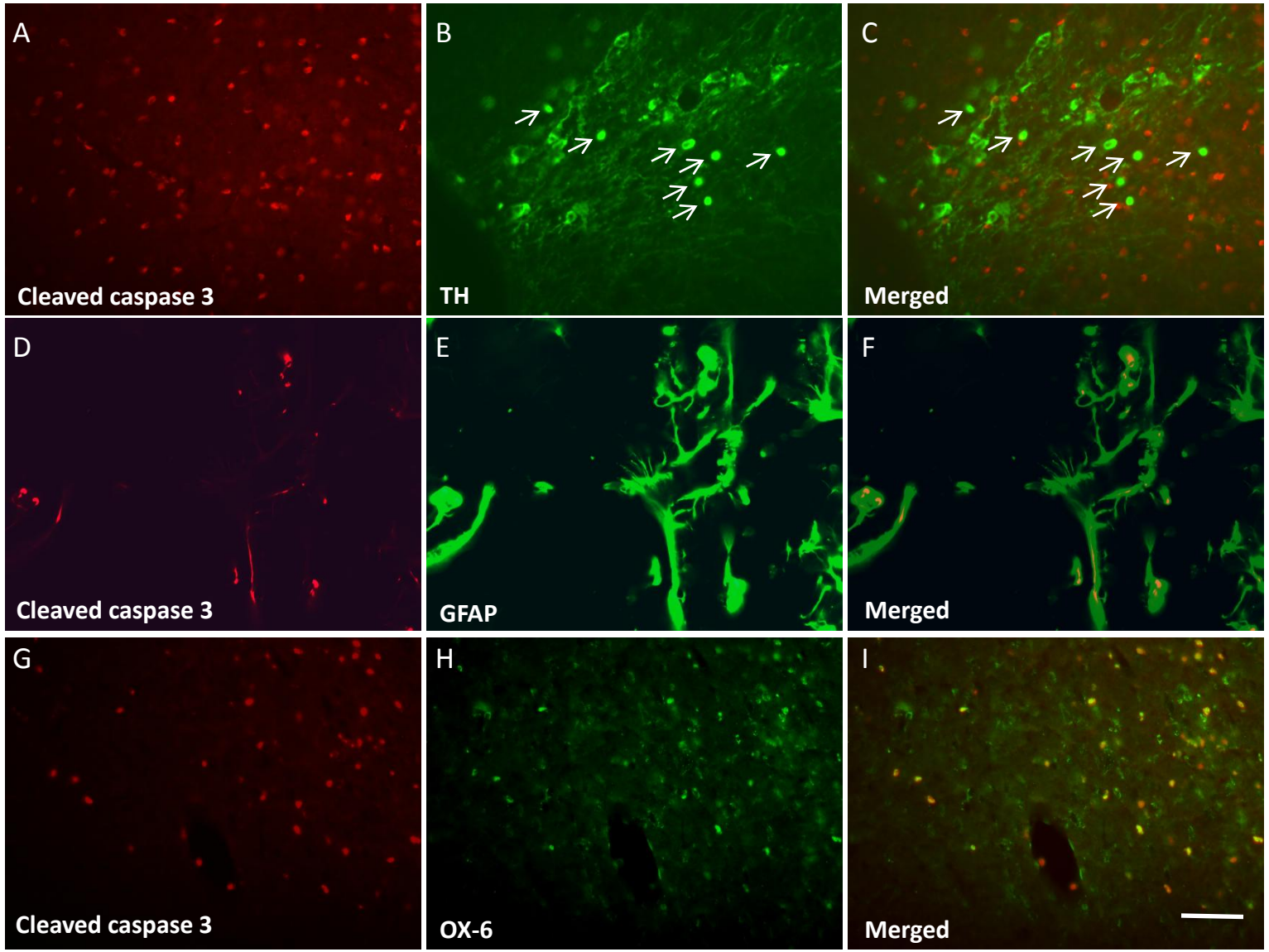

Figure 2. Burguillos et al

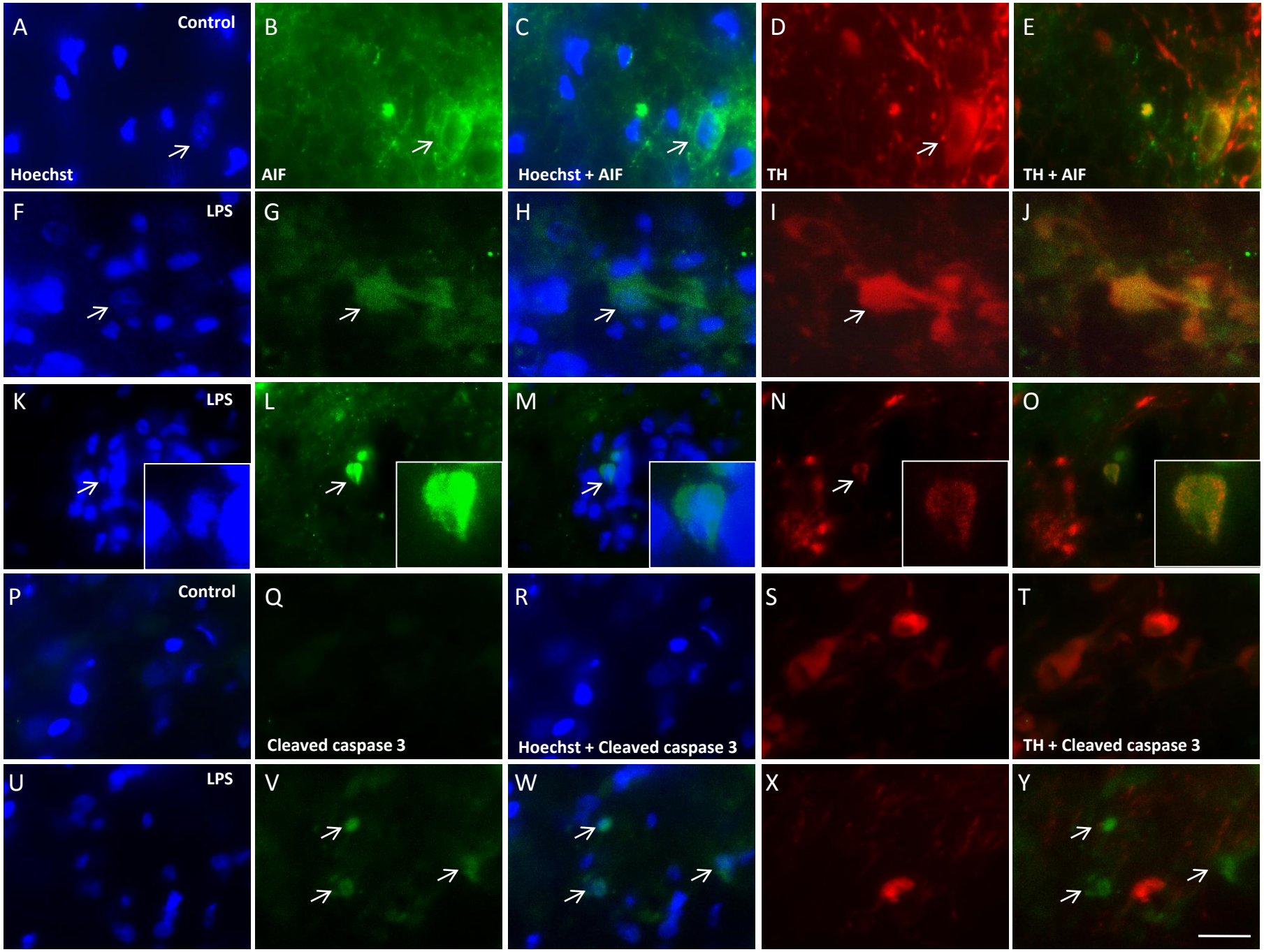

Figure 3. Burguillos et al

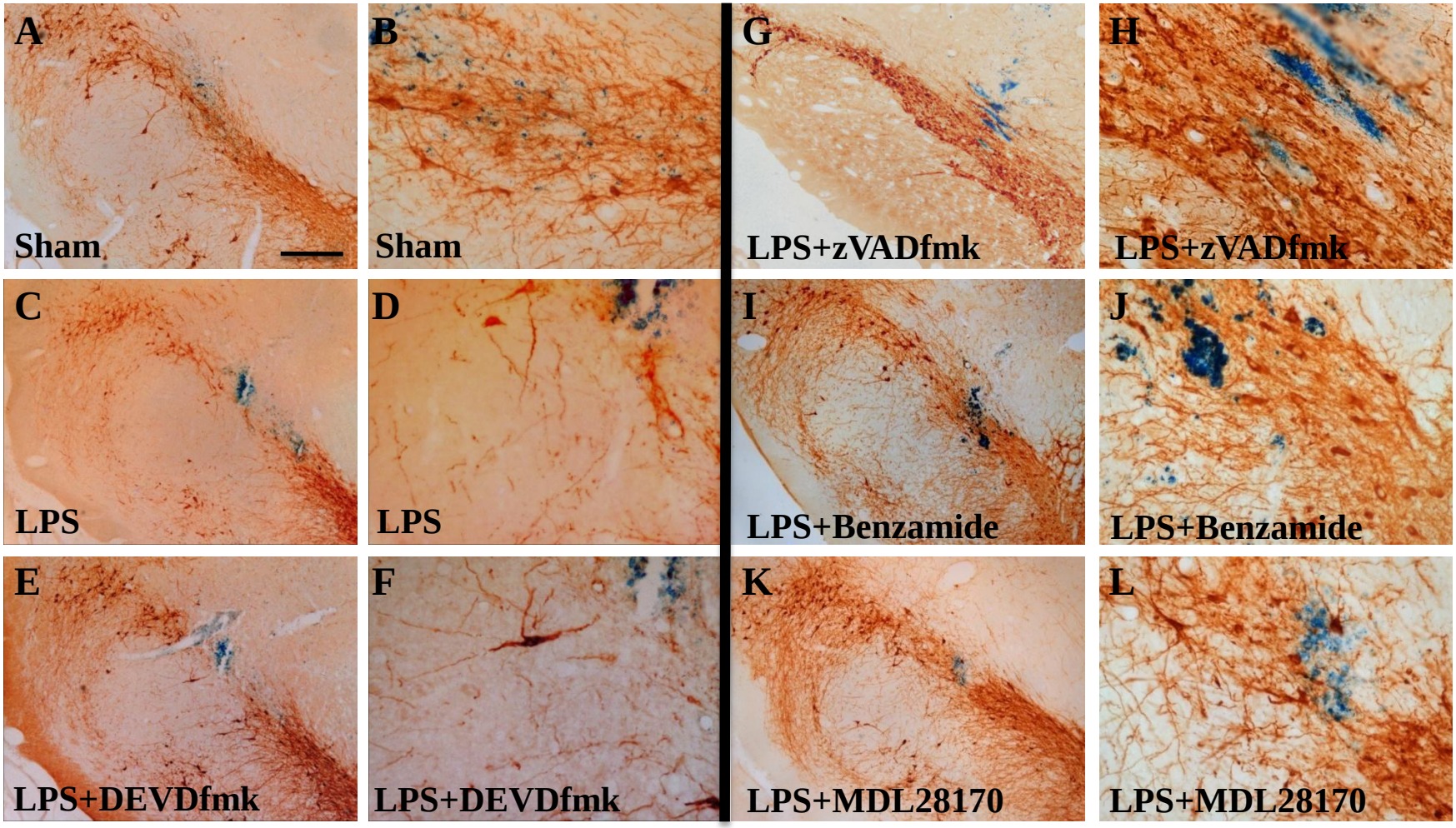

Figure 4. Burguillos et al

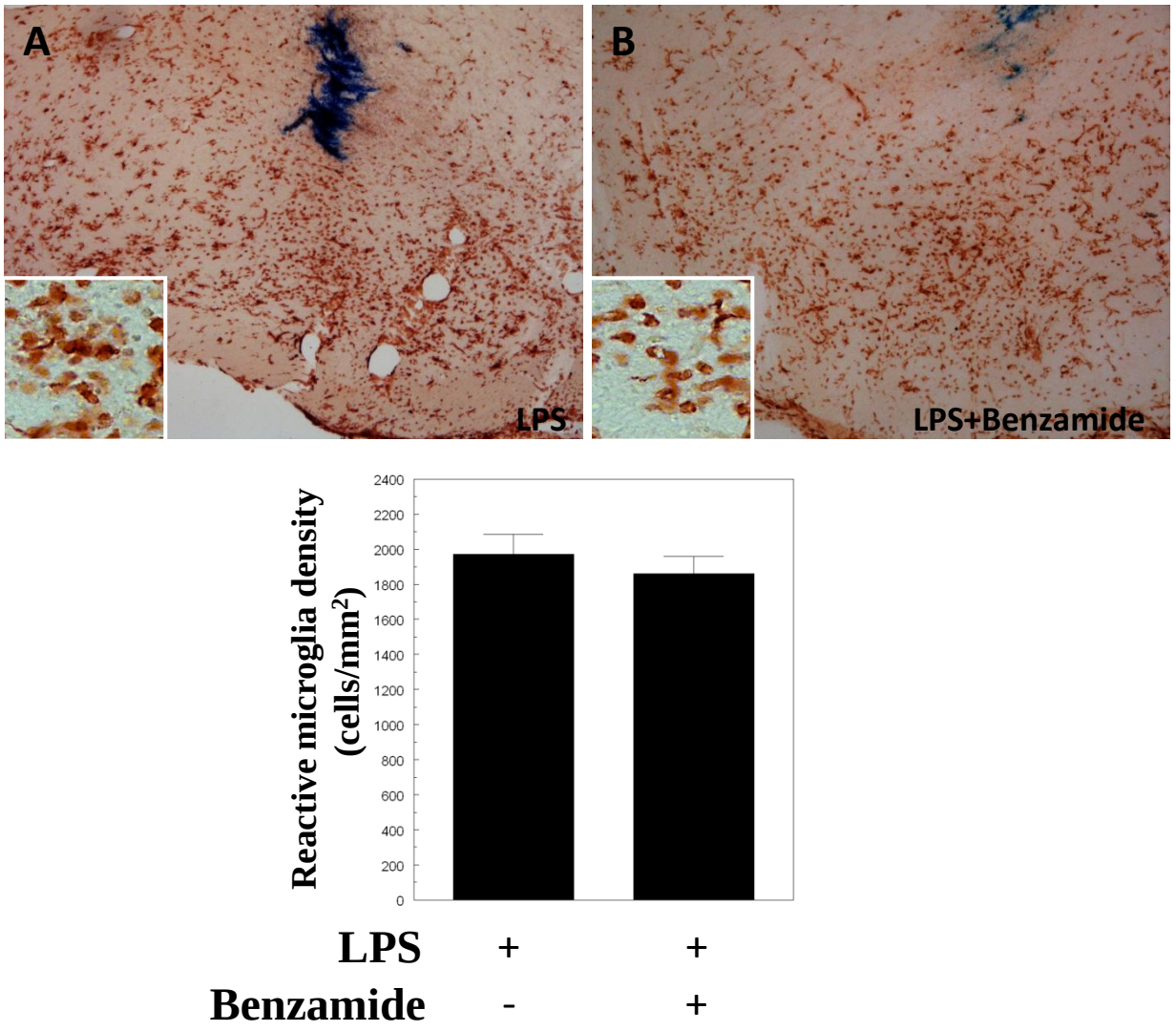

Figure 5. Burguillos et al

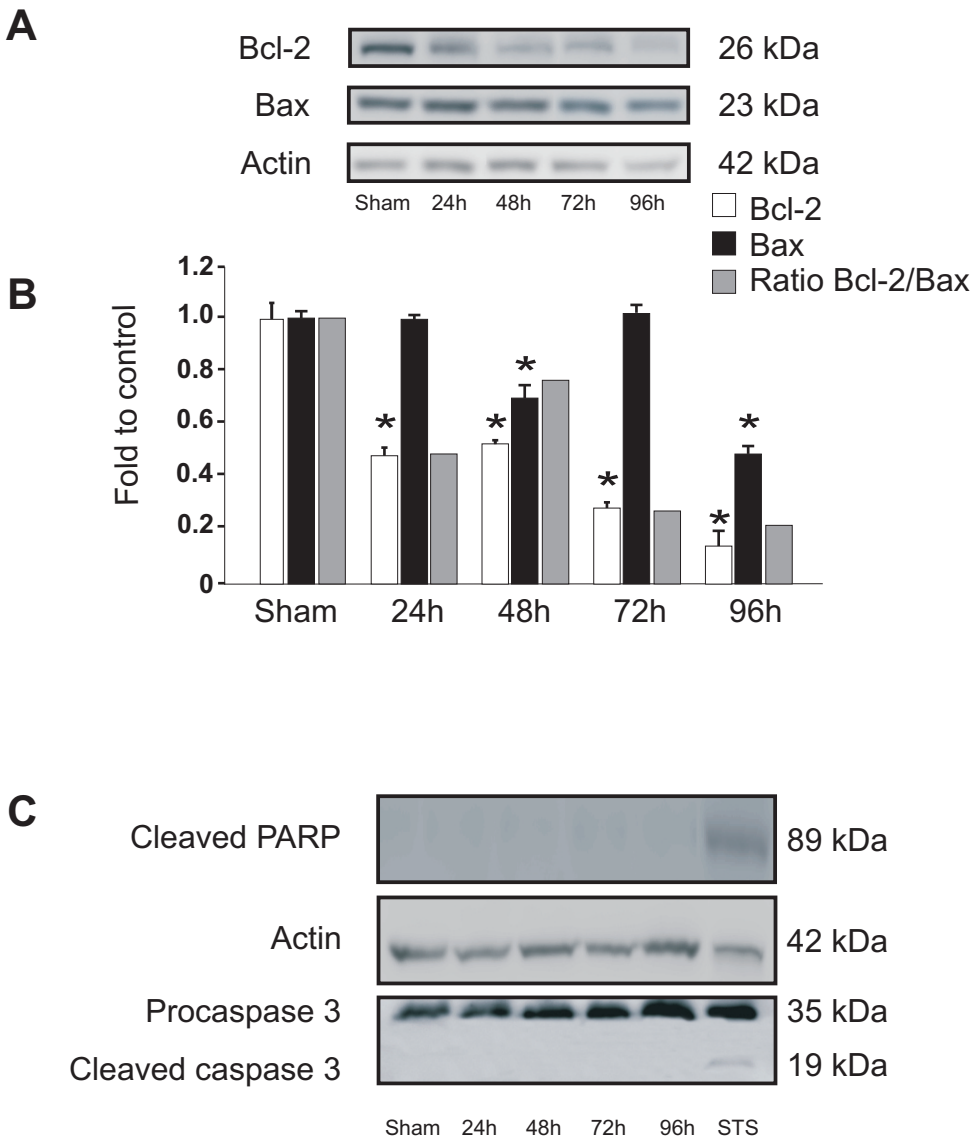

Fig. 1 Burguillos et al.

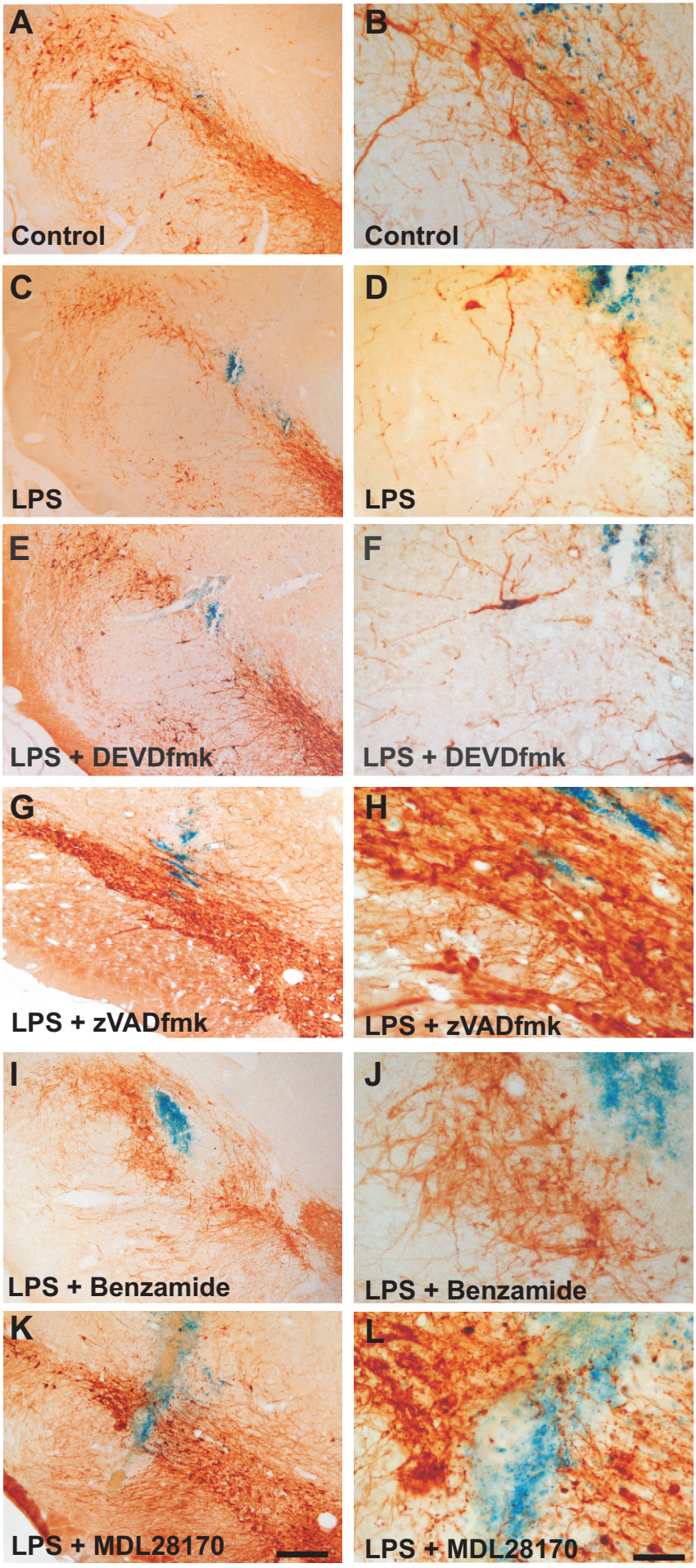

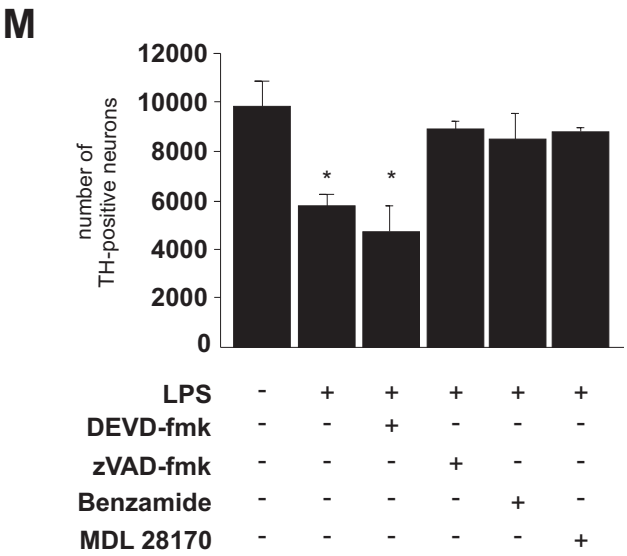

Fig. 5 Burguillos et al.

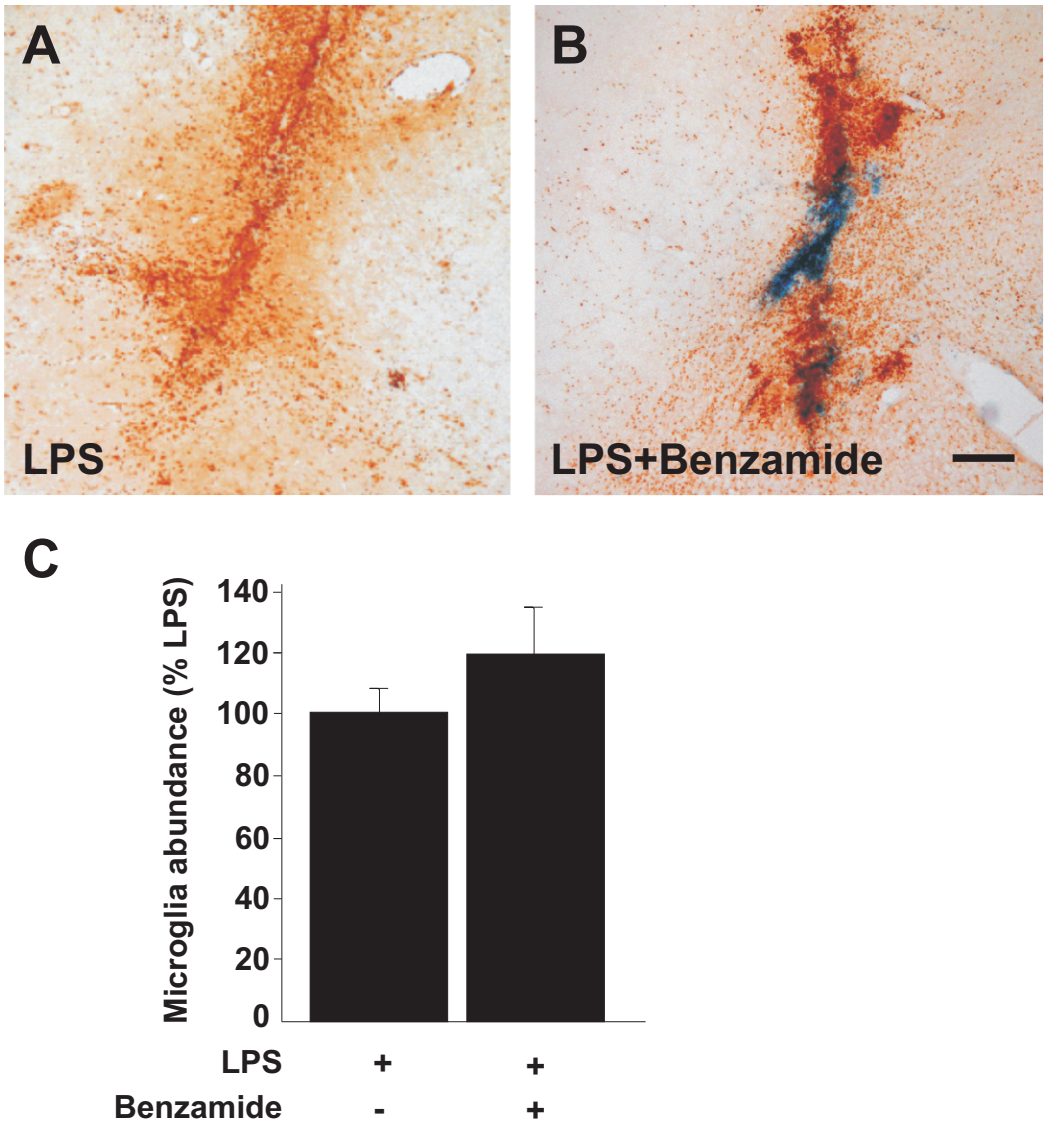

Fig. 6 Burguillos et al.

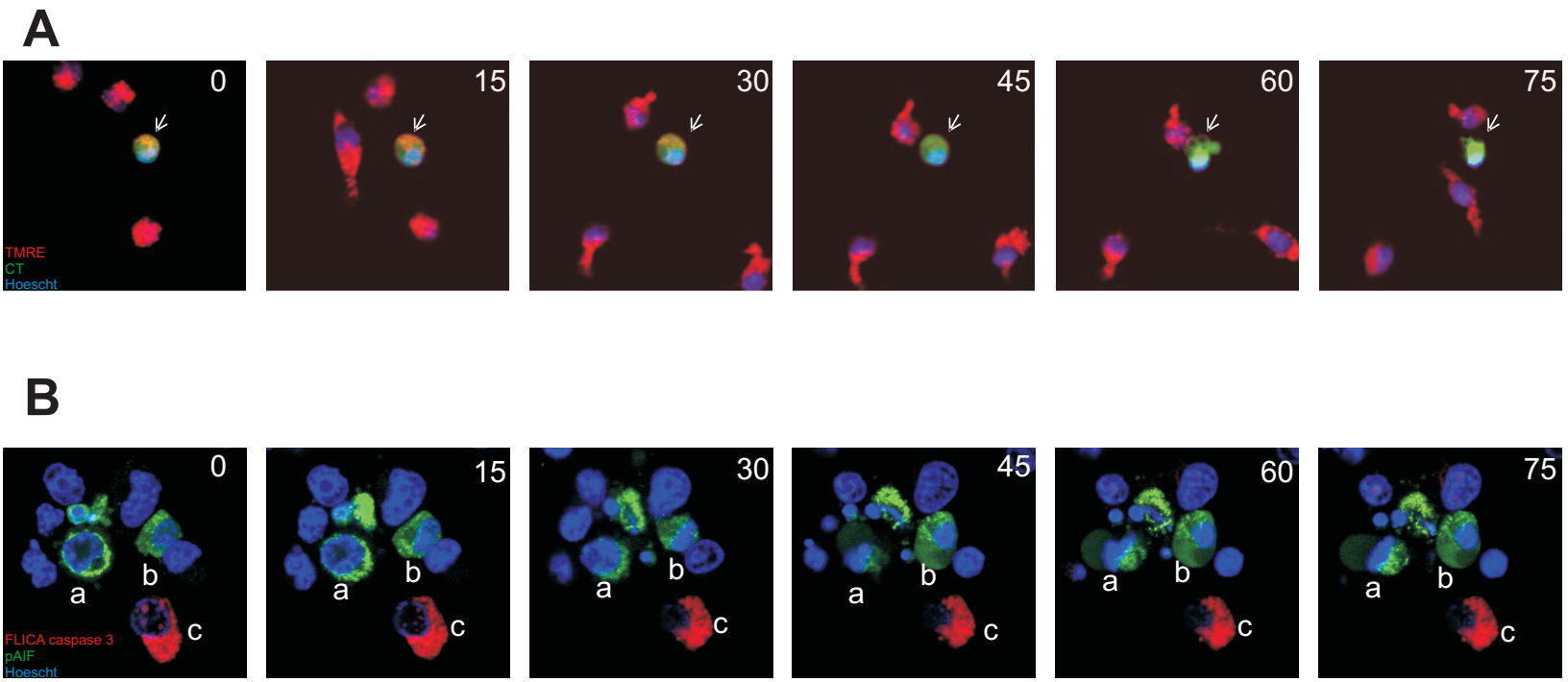

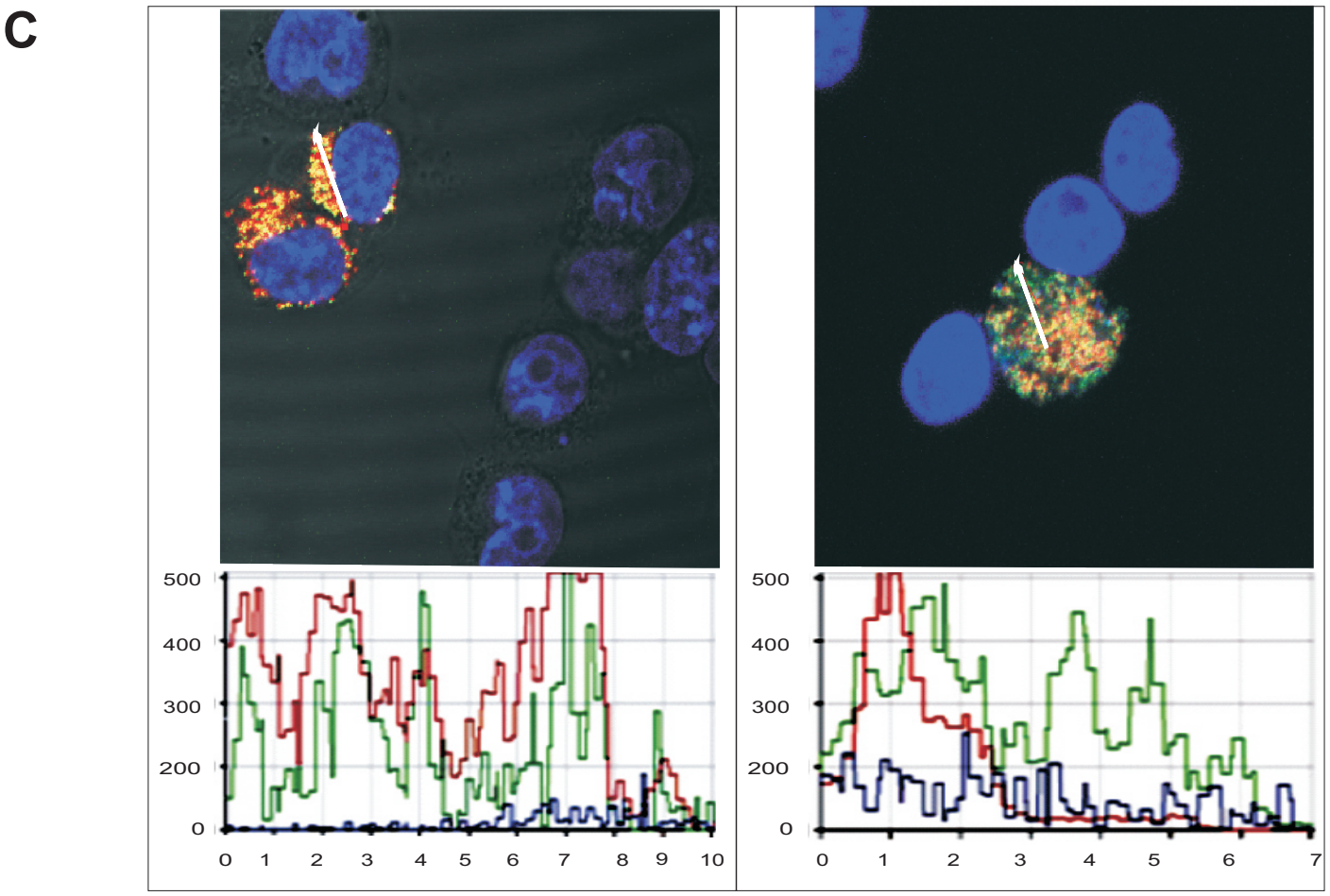

Figure 6. Burguillos et al.

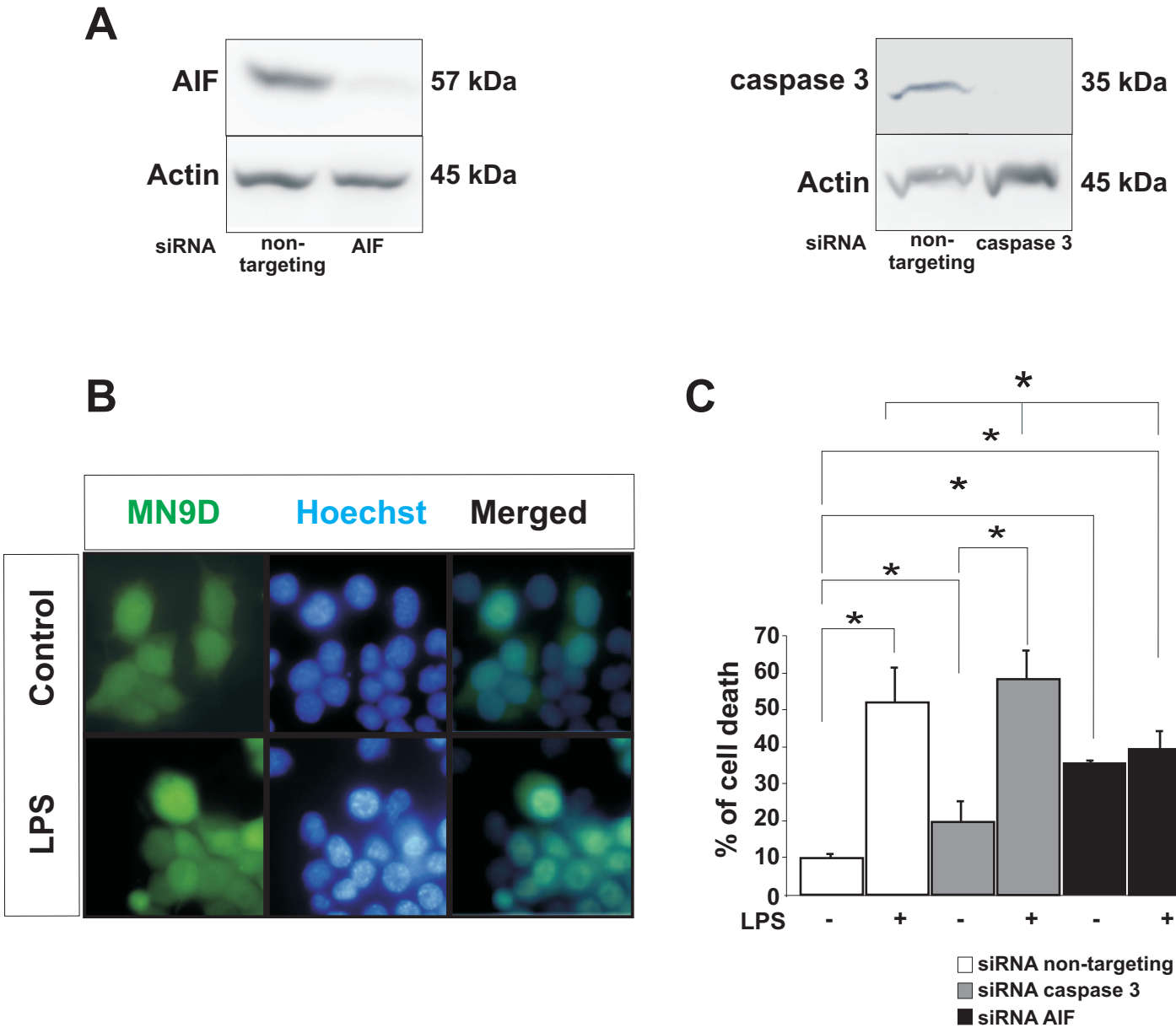

Fig. 8 Burguillos et al.

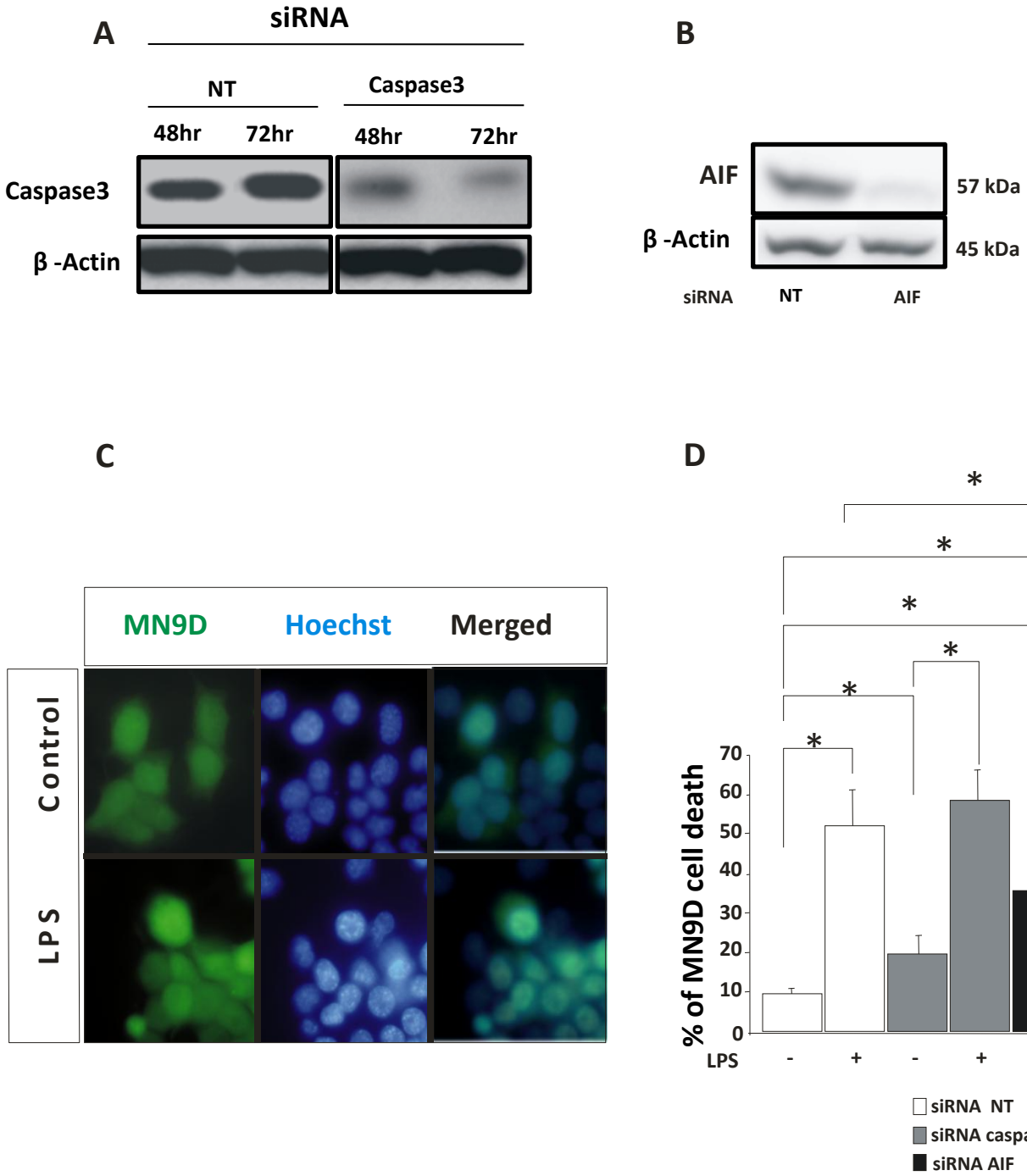

Figure 7. Burguillos et al

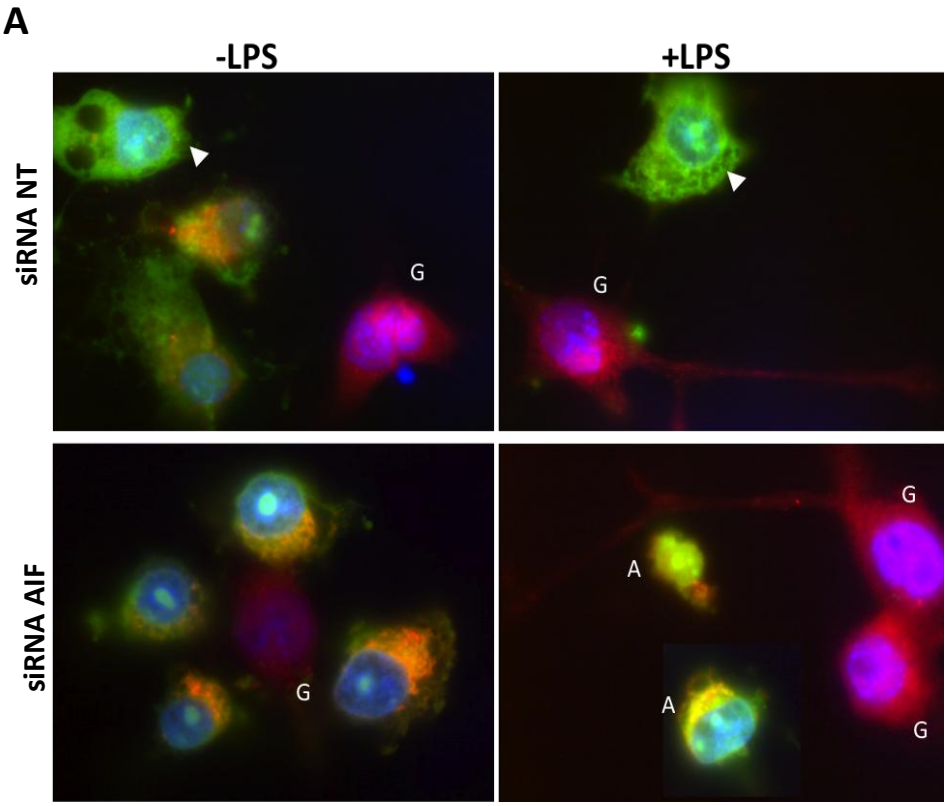

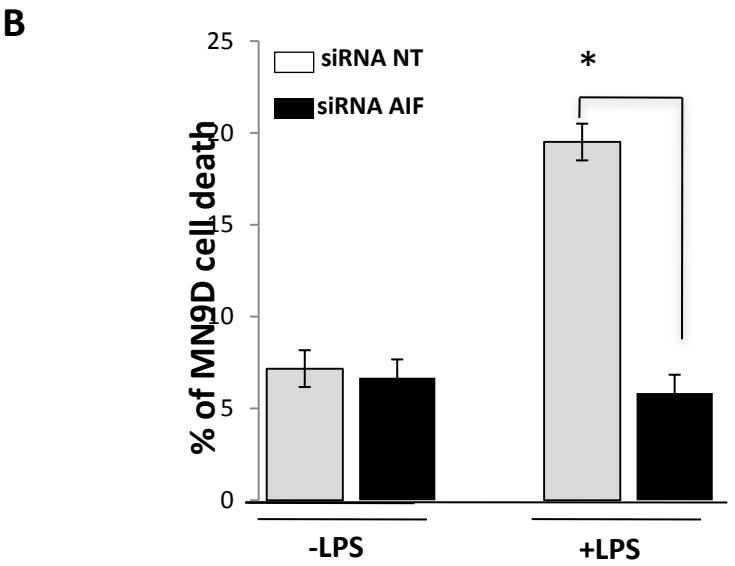

Figure 8. Burguillos et al

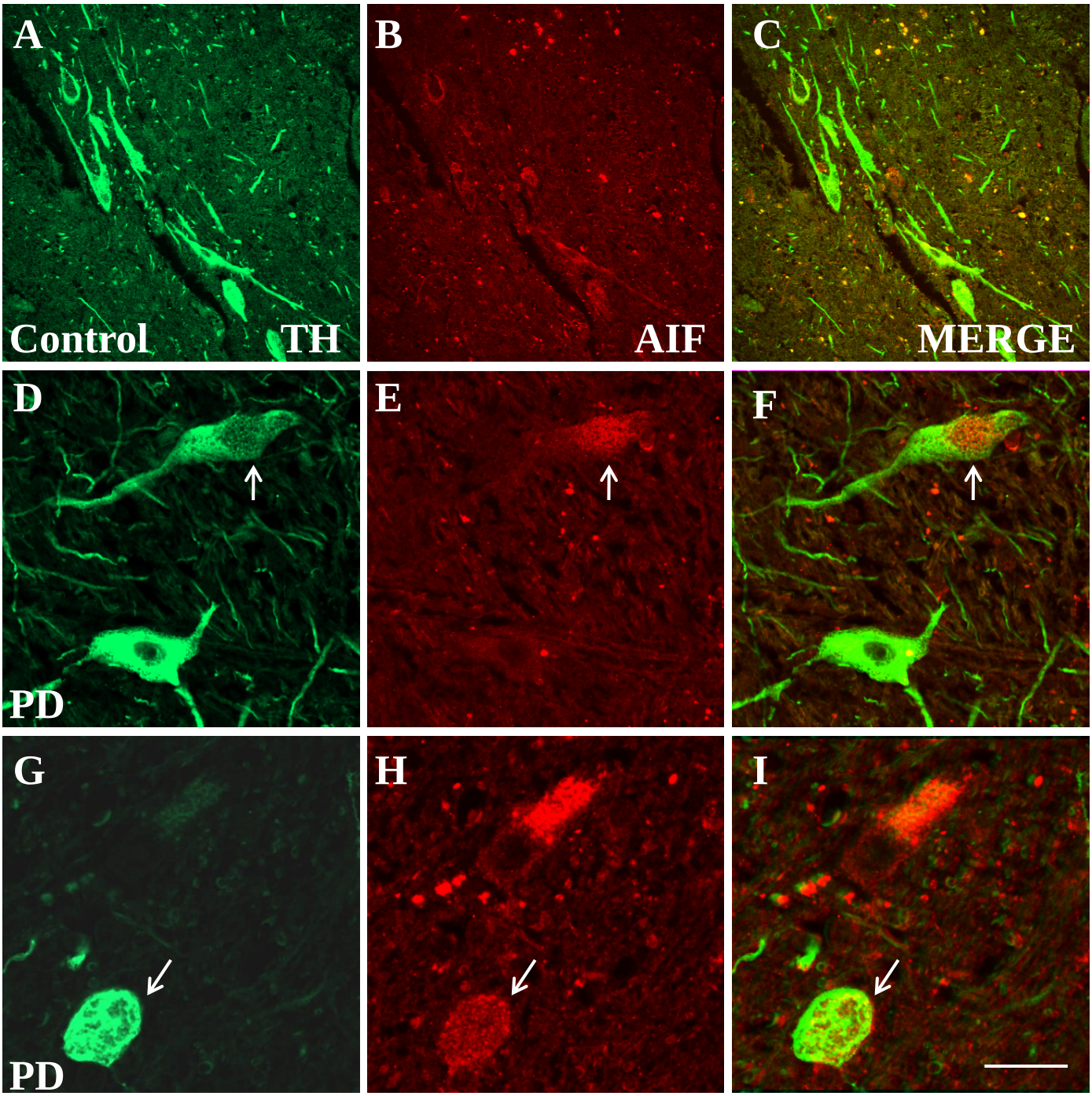

Figure 9. Burguillos et al

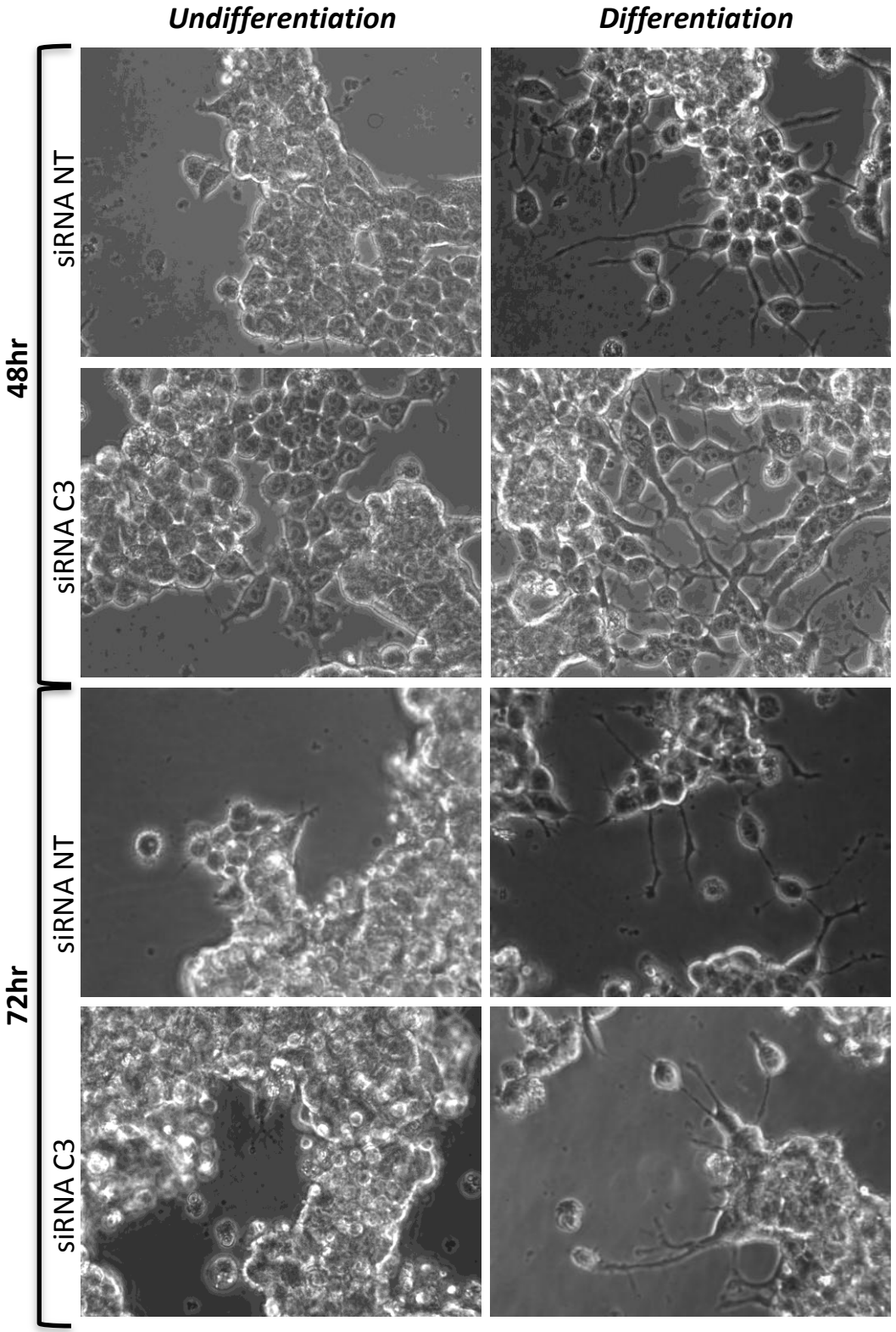

Suppl. Figure 1. Burguillos et al